

Analyzing and Predicting CAT Bond Premiums: a Financial Loss Premium Principle and Extreme Value Modeling

Gilles Stupfler^[a] Fan Yang^{[b]*}

^[a]School of Mathematical Sciences, University of Nottingham
University Park, Nottingham NG7 2RD, United Kingdom

^[b]Department of Statistics and Actuarial Science, University of Waterloo
Waterloo, ON N2L 3G1, Canada

August 17, 2017

Abstract

CAT bonds play an important role in transferring insurance risks to the capital market. It has been observed that typical CAT bond premiums have changed since the recent financial crisis, which has been attributed to market participants being increasingly risk-averse. In this work, we first propose a new premium principle, the financial loss premium principle, which includes a term measuring losses in the financial market that we represent here by the Conditional Tail Expectation (CTE) of the negative daily log-return of the S&P 500 index. Our analysis of empirical evidence suggests indeed that in the post-crisis market, instead of simply increasing the fixed level of risk load universally, the increased risk aversion should be modeled jointly by a fixed level of risk load and a financial loss factor to reflect trends in the financial market. This new premium principle is shown to be flexible with respect to the confidence/exceedance level of CTE. In the second part, we focus on the particular example of extreme wildfire risk. The distribution of the amount of precipitation in Fort McMurray, Canada, which is a very important factor in the occurrence of wildfires, is analyzed using extreme value modeling techniques. A wildfire bond with parametric trigger of precipitation is then designed to mitigate extreme wildfire risk, and its premium is predicted using an extreme value analysis of its expected loss. With an application to the 2016 Fort McMurray wildfire, we demonstrate that the extreme value model is sensible, and we further analyze how our results and construction can be used to provide a design framework for CAT bonds which may appeal to (re)insurers and investors alike.

1 Introduction

Catastrophic events are a major source of concern for insurance markets and companies: in the case of climate-related events, their number has followed a positive trend in recent years; see Hoeppe (2016). A single such event may cause billions of dollars worth of losses in total: for example, Hurricane Katrina with a loss of \$84 billion, the 2008 Sichuan earthquake in China for \$148 billion, the 2011 Tōhoku earthquake and tsunami in Japan for over \$300 billion, Hurricane Sandy for \$75 billion, and the most recent 2016 Fort McMurray wildfire with an estimated loss of \$3.58 billion which makes it the most expensive disaster in Canadian history. Catastrophe (CAT) bonds pay regular coupons to investors and the principal is contingent on a predetermined catastrophic

*Corresponding author: fan.yang@uwaterloo.ca

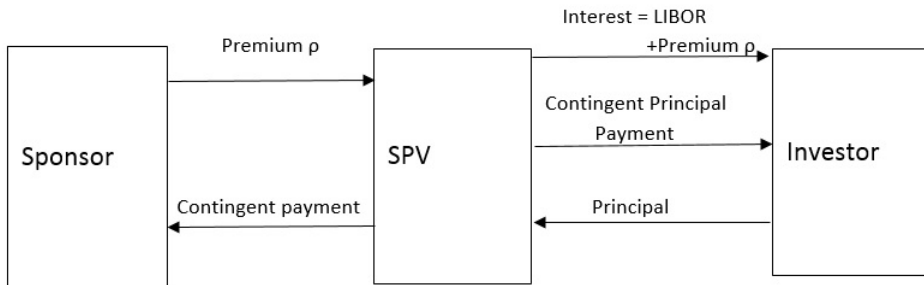


Figure 1: A CAT bond transaction

event defined in the bond indenture. This type of insurance-linked securities (ILS) has grown substantially in the past two decades and it has a high record of over \$25 billion outstandings in 2014. It is safe to say that CAT bonds have become an alternative to transfer insurance risks to the capital market.

As shown in Figure 1, a typical CAT bond transaction involves three parties. In order to protect themselves from big losses consecutive to catastrophic events, the sponsor, which is usually an insurer or reinsurer, purchases a reinsurance contract with a Special Purpose Vehicle (SPV). In this contract, the sponsor pays a premium ρ to receive a contingent payment from the SPV. If there is no trigger event during the term, the SPV makes no payment to the sponsor at maturity. If there is a trigger event, the SPV makes a payment up to a limit to the sponsor to cover the loss due to the catastrophic event. On the other hand, to ensure the payment, the SPV sells a CAT bond to investors, who expect to receive high yields from the CAT bond and diversify their portfolios. The coupon rate is usually LIBOR plus the premium. At maturity, depending on the occurrence of the trigger event, the investor receives all, part or even none of the principal back. The most commonly and widely used type of trigger is the indemnity. Because it usually takes a long time after a catastrophic event to determine the actual loss and a quick settlement is generally not possible, CAT bonds with indemnity trigger have higher basis risks and moral hazards. A parametric trigger, meanwhile, uses a physical measure, which can be obtained accurately and immediately after a catastrophic event. In general, nonindemnity triggers introduce basis risk to the sponsor but eliminate the moral hazard for the investor. With a trade-off between basis risk and moral hazard, CAT bonds with indemnity triggers can be expected to have higher premiums (see *e.g.* Cummins and Weiss, 2009) although there is an ongoing debate as to whether this is always verified empirically (see Gurtler *et al.*, 2016).

Since CAT bonds are quoted using their premiums, or equivalently their spreads over LIBOR in the market, the premium is sometimes referred to as the price of a CAT bond. In this paper, we focus on the econometric approach to pricing, which concentrates on the relationship between the CAT bond premium and the determining factors based on empirical analyses. Lane (2000) is probably the first paper using CAT bond primary market data to link the premium and the expected loss by a power function. Multiple factor linear models have been used in Lane and Mahul (2008) and Braun (2016). Galeotti *et al.* (2013) compared the fit of the linear model, of the log-linear model used in Major and Kreps (2002) and of Wang's distortion in Wang (2004). They concluded that without taking the 2008 financial crisis into account, the Wang transformation and the linear premium model are the most accurate ones.

Empirical studies have shown that the financial crisis has had a significant impact on CAT

bonds; see for example Carayannopoulos and Perez (2015) and Gurtler *et al.* (2016). In the first part of this paper, and through the study of the 2004 to 2014 primary CAT bond market, we will show that CAT bond premiums have indeed been strongly correlated with the financial market since the financial crisis, and our estimates point to a correlation 50% higher than pre-crisis, an increase that we attribute to investors becoming increasingly risk averse. However, we would not conclude that CAT bond premiums have increased after the crisis. In fact, summary statistics of the data show that the median premium has slightly increased, while the average premium has slightly decreased. We then show that there is significant evidence of a structural break in the price structure corresponding to the financial crisis. These reasons motivated us to introduce a new premium principle, which we call the *financial loss premium principle* in this paper and that, in addition to the expected loss, takes financial losses into account through a Conditional Tail Expectation (CTE) of the negative daily log-return of the S&P 500. We find that, in the post-crisis period, this new premium principle recovers a quantity of information equivalent to the one lost by the linear premium model after the financial crisis, and its goodness-of-fit is stable with respect to the confidence/exceedance level of CTE.

An explanation put forward by Gurtler *et al.* (2016) regarding such changes in CAT bond premium models is that investors now mistrust the expected loss calculated by catastrophe modeling companies. Generally, standard statistical methods are not efficient enough to study catastrophic risks due to the scarcity of observations. Extreme Value Theory (EVT) provides an adapted way to investigate catastrophic risks with a moderate amount of data. Briefly, EVT allows one to, under a condition called the Maximum Domain of Attraction (MDA) condition, approximate the distribution of the highest values in the sample by either the Generalized Extreme Value (GEV) or Generalized Pareto (GP) distributions through two different techniques: the block maxima model and the Peaks-Over-Threshold (POT) approach. The MDA covers a wide range of commonly used distributions which are especially appropriate to capture extreme risks. Moreover, the efficient use of the data by the POT method together with the simplicity of the GP distribution generally gives EVT great flexibility to analyze the right tail of a data set. Much research has showed the effectiveness of EVT in estimating the likelihood of natural hazards or catastrophic losses; see for example Beirlant *et al.* (1996), Simiu and Heckert (1996), McNeil and Saladin (1997), Rootzen and Tajvidi (1997), Alvarado *et al.* (1998), Koutsoyiannis (2004) and Zimbidis *et al.* (2007).

In the second part of the paper, and in order to provide an improvement upon current practice in the calculation of expected losses, we provide predictive pricing models under EVT assumptions. Indeed, since CAT bonds usually cover the last layer of loss, the expected loss crucially depends on the attachment point, which is the level that the loss must exceed so that the coverage is triggered, and the exhaustion point, which defines the maximum coverage of the contract. The idea of CAT bonds being to insure against catastrophic events, one may consider both points to be high but it is important to know how high they should be, and also how the choices of these two points affect the premium. We then derive asymptotic equivalents of the linear premium and financial loss premium principles, respectively, when the layer is high under a general EVT condition on the trigger variable. The asymptotic expressions are simple and provide valuable insight regarding the behavior of the premium for high attachment and exhaustion points at the designing stage of a CAT bond.

In the final part of the paper, we focus on the example of extreme wildfire risk, and in particular on the 2016 Fort McMurray wildfire. This disaster highlighted that a better risk management system is urgently needed for extreme wildfire risk. We tackle this problem using a two-step approach. Because wildfires often occur during the summer and following a dry fall and winter and warm spring, we recognize that the amount of precipitation in the fall, winter and spring seasons is a very important contributing factor to wildfires in the summer season. In other words,

precipitation is a good candidate for a parametric trigger in a wildfire CAT bond. By applying the POT method of EVT, we first fit a GP distribution to (transformed) low precipitation data collected in Fort McMurray. Second, once the distribution of low precipitation has been estimated, we design a wildfire bond whose parametric trigger is the aggregated amount of precipitation in the nine months before a given summer season, and we apply this construction to the example of the 2016 Fort McMurray wildfire. We further illustrate how the financial loss premium compares to the linear premium on this situation.

The rest of the paper consists of five parts. In Section 2, through the study of real CAT bond data, we analyze the structural change of CAT bond premiums due to the financial crisis, and then propose our new premium principle for a better fit of the post-crisis market. In Section 3, we carry out an asymptotic analysis of the linear and financial loss premium models. In Section 4, a GP distribution is fitted to a transformed sample of data for low precipitation in Fort McMurray using the POT method, and we construct and analyze empirically a nine-month wildfire bond with precipitation trigger. A conclusion then summarizes the contribution of this work. All proofs are postponed to the Appendix.

2 The financial loss premium principle

In the pricing of CAT bonds, the expected loss (EL) is undoubtedly the most important factor; see Froot (2001) for example. Before defining the EL, we start with some related concepts. Let a nonnegative random variable L represent the catastrophic risk. With an attachment point t and an exhaustion point h , the loss related to this layer is

$$L_{(t,h]} = \begin{cases} 0, & \text{if } L \leq t, \\ L - t, & \text{if } t < L \leq h, \\ h - t, & \text{if } L > h. \end{cases}$$

The payoff rate of a CAT bond covering this layer of loss, denoted by a random variable Z , is given by

$$Z = \frac{(L - t)_+ - (L - h)_+}{h - t}.$$

The expected loss EL is defined as the average value of Z :

$$\text{EL} = \text{E}[Z] = \frac{\text{E}[(L - t)_+] - \text{E}[(L - h)_+]}{h - t}.$$

From this definition, EL is actually the average percentage of the maximum payment $h - t$ which is not paid back to the investor and kept by the sponsor at maturity.

Due to the exposure to uncertain losses, the CAT bond premium usually consists of two parts, expected loss and risk loading. Generally, a premium principle can be expressed as

$$\rho(L) = \text{EL} + \Lambda,$$

where Λ represents the risk loading. The linear premium principle proposed in Lane and Mahul (2008), which roots from the expected value principle, is defined as

$$\rho_{\text{linear}}(L) = a + b \text{EL}, \quad \text{for } a, b > 0. \quad (2.1)$$

As Lane and Mahul (2008) point out, a value of b larger than 1 means part of the risk loading Λ is from the EL, and this will indeed be the case in our data as our statistical analysis will show.

In this section, and although we shall make this clearer later, let us mention that two models for Λ will be examined: besides the portion $(b - 1)EL$, we compare the linear premium principle with a fixed level of risk load a as in (2.1), to our new model (see (2.4) below) incorporating a further factor measuring risk loading through financial tail risk. Other possible models would be to include part of the load in additional “central” (*i.e.* non-tail) dispersion indicators such as variance or standard deviation (see *e.g.* Chapter 4 of Bühlmann, 1970 in classical pricing contexts); this is not our purpose here, since we specifically want to assess the effect of tail risk on CAT bond premiums. Let us also point out that, according to Galeotti *et al.* (2013), the linear premium principle is the most accurate principle which does not take the 2008 financial crisis into account. This motivated us to build our premium principle upon the linear premium, and the latter will then be used as a benchmark for goodness-of-fit in this section.

Since our focus in this section is on pricing models for CAT bonds, we recall that past studies, including Carayannopoulos and Perez (2015) and Gürtler *et al.* (2016), have observed that the price structure of CAT bonds has changed since the financial crisis, which suggests that there is a significant correlation between financial losses and CAT bond premiums. We first check this by using 10 years’ primary CAT bond market data and S&P 500 data. The CAT bond data we consider here have been obtained from the primary ILS data provided by Lane Financial LLC. After cleaning the data, for example removing all non-catastrophic risk related ILSs and any implausible entries or any entries with missing terms, there are 375 CAT bond tranches from the second quarter of 2004 to the first quarter of 2014. The information for each CAT bond entry includes the (adjusted spread) premium ρ , the expected loss EL, the probability of first loss (PFL = $\Pr(L > t)$), the probability of last loss (PLL = $\Pr(L > h)$), issue date and maturity. To test for correlation between CAT bond premiums and financial losses, we take the average of the negative daily log-returns of S&P 500 over the 12 months preceding the issue date of the bond as the indicator of financial loss. Let us recall that the log-return on day i is defined as $\log(p_i/p_{i-1})$, with p_j denoting the price on day j , and the negative daily log-return we consider in our analysis is simply minus this value, namely $\log(p_{i-1}/p_i)$. The reason why we choose an average over 12 months is that a one-year period is long enough to capture recent extreme movements in the market and thus assess their influence, while it is short enough to suppress the influence of any long-term trend or dependence.

To analyze first the impact of the financial crisis on the CAT bond market, the whole CAT bond data set 2004-2014 is separated into two periods: the pre-financial crisis period 2004-2007 which is called “pre-crisis” and the financial crisis-affected period 2008-2014 which is called “post-crisis” for the sake of simplicity (although the range does not cover the very latest years of the post-crisis period). Summary statistics of the premium, EL, and one-year average negative daily log-return of S&P 500 in the pre- and post-crisis period are given in Table 1. We note that there is an increase of the minimum and median premiums and a decrease of the maximum and mean premiums in the post-crisis period compared to the pre-crisis period, and as such we would not conclude that actual premium values have generally increased after the financial crisis.

Our goal is now to assess if CAT bond premiums are correlated with movements in the financial market, and especially if this potential correlation increased after the financial crisis. With the help of the R function `cor.test`, we reject the hypothesis that financial losses have zero correlation with CAT bond premiums for the whole CAT bond data set from 2004 to 2014. A similar conclusion is reached by Gürtler *et al.* (2016), although they use standard quarterly returns of the S&P 500. The correlation during the post-financial crisis period 2008-2014 is estimated to be 50% higher than the correlation in the whole data set or the pre-crisis period. The results are summarized in Table 2 below.

This estimated increasing correlation suggests that the financial crisis has indeed had an impact

Pre-crisis	Variable	Minimum	25% quantile	Median	Mean	75% quantile	Maximum
	Premium	0.00660	0.04423	0.07100	0.09152	0.11278	0.49880
	EL	0.00010	0.00778	0.01295	0.02310	0.03455	0.12750
	S&P return	-0.000755	-0.000499	-0.000364	-0.000413	-0.000294	-0.000116
Post-crisis	Variable	Minimum	25% quantile	Median	Mean	75% quantile	Maximum
	Premium	0.01770	0.05400	0.08110	0.08637	0.11410	0.22310
	EL	0.00010	0.00890	0.01570	0.02113	0.02795	0.13060
	S&P return	-0.001656	-0.000757	-0.000380	-0.000269	-0.000057	0.00236

Table 1: Summary statistics of the premium, EL, and one-year average of negative daily log-returns of S&P 500 in the pre- and post-crisis period.

	t value	p -value	95% CI	Sample correlation
Global data	3.7385	0.0002141	(0.0905, 0.2858)	0.1900
Pre-crisis data	2.3694	0.01912	(0.03208, 0.3431)	0.1924
Post-crisis data	4.6346	$6.059e - 06$	(0.1716, 0.4097)	0.2952

Table 2: Sample correlation between financial losses and CAT bond premiums.

on the structure of CAT bond prices. To assess this impact, and recalling that Galeotti *et al.* (2013) showed that the linear premium principle is the most accurate principle which does not take the 2008 financial crisis into account, we start then by examining the presence of a change point in the linear premium model at the time of the financial crisis. Since the CAT bond data set comes from a time series, autocorrelation should be accounted for; indeed, standard regression testing when the independence assumption of the errors is violated very often results in higher t values and lower p -values, potentially leading us to conclude that there is significant evidence for the existence of relationships in the data that are actually nonexistent. In Figure 2, we plot the autocorrelation functions (ACF) for the residuals of the linear premium principle model in the whole, pre-crisis and post-crisis period considered.

Figure 2 shows that there is indeed evidence of sizeable autocorrelation in the data. Hence, we use heteroskedasticity- and autocorrelation-resistant testing; the estimators remain the ordinary least squares estimators but testing is done by replacing the usual denominators in the t -statistics by suitable estimators of the true variance. The variance is estimated by the Andrews (1991) version of the Newey-West (1987) estimator. We apply these adapted robust regression techniques to fit the linear premium principle for three data sets: the whole data set, the data set corresponding to the pre-crisis period and the one corresponding to the post-crisis period. Results are reported in Table 3.

Results seem to indicate a change in the slope b of the regression model between the pre- and post-crisis periods, as well as a loss of explanatory power in the post-crisis period, indicated by a smaller R^2 . These two observations suggest that there exists a structural break in the regression model, and more specifically that the linear premium principle does not fit the post-crisis data as well as it fits the pre-crisis data. To accurately test whether there is indeed a significant change in the slope b between the two periods, we use the following model:

$$\rho(L) = a + b \text{EL} + c \text{Ind} + d \text{EL} \times \text{Ind}, \quad (2.2)$$

where Ind is the dummy variable 0 in pre-crisis and 1 afterwards. In other words, $\rho(L) = a + b \text{EL}$ in the pre-crisis period, and $\rho(L) = (a + c) + (b + d) \text{EL}$ in the post-crisis period. A structural

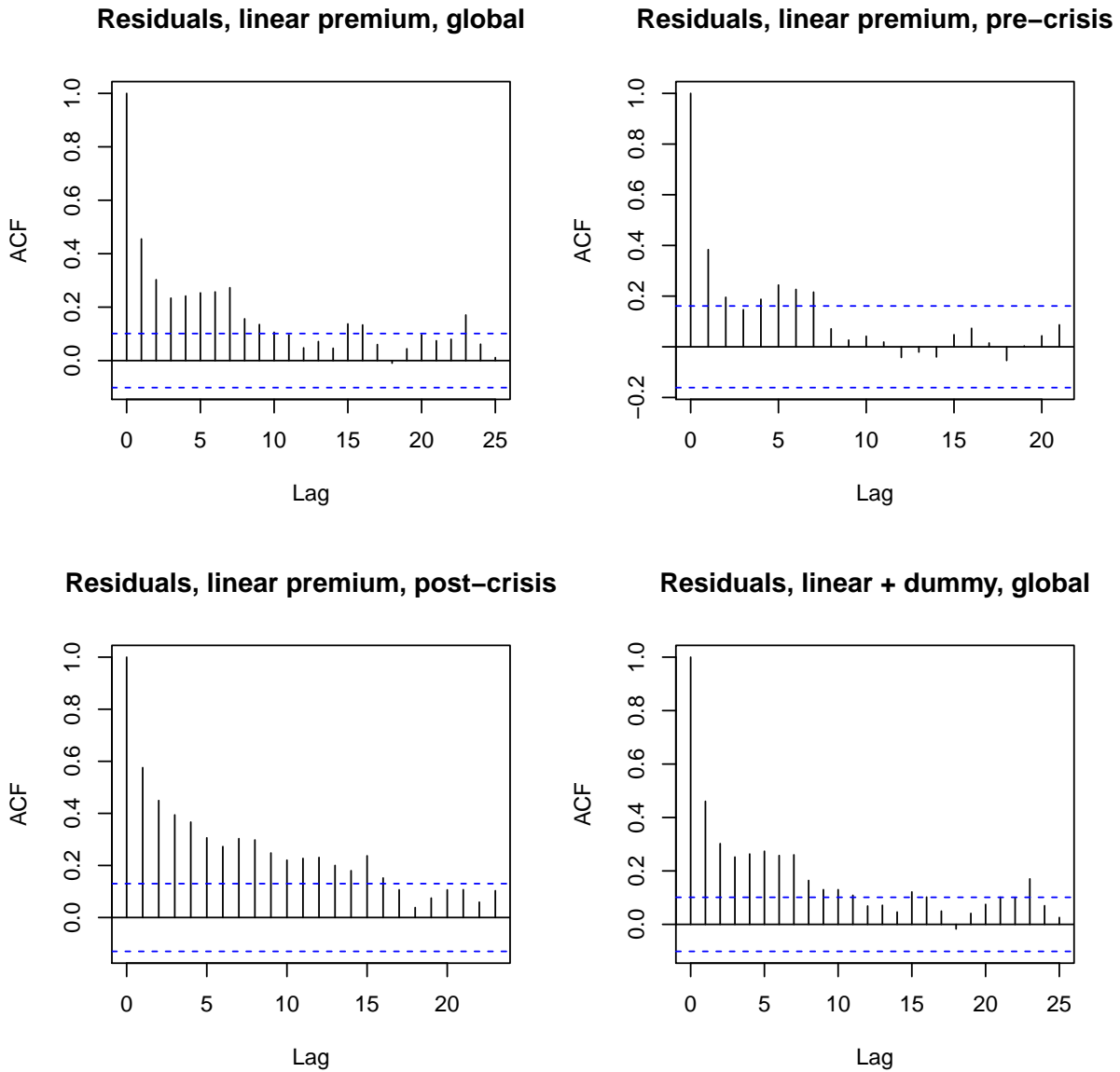


Figure 2: ACFs of the residuals. Top left: global regression model (2004-2014) $\rho(L) = a + bEL$, top right: pre-crisis model (2004-2007) $\rho(L) = a + bEL$, bottom left: post-crisis model (2008-2014) $\rho(L) = a + bEL$, bottom right: global regression model (2004-2014) $\rho(L) = a + bEL + cInd + dEL \times Ind$ with the dummy variable Ind indicating the financial crisis.

Global	Coefficients	Estimate	Std. error	t value	p -value	Adj. R^2 0.6433
	a	0.03900	0.003522	11.076	$< 2.2e - 16^{***}$	
	b	2.2550	0.1805	12.491	$< 2.2e - 16^{***}$	
Pre-crisis	Coefficients	Estimate	Std. error	t value	p -value	Adj. R^2 0.7071
	a	0.03020	0.003959	7.6301	$2.787e - 12^{***}$	
	b	2.6548	0.2254	11.7789	$< 2.2e - 16^{***}$	
Post-crisis	Coefficients	Estimate	Std. error	t value	p -value	Adj. R^2 0.5789
	a	0.04838	0.004045	11.961	$< 2.2e - 16^{***}$	
	b	1.7982	0.1529	11.761	$< 2.2e - 16^{***}$	

Table 3: Regression results for the linear principle (2.1)

No correction	Coefficients	Estimate	Std. error	t value	p -value
	a	0.03020	0.003868	7.8090	$5.963e - 14^{***}$
	b	2.6548	0.1154	23.005	$< 2.2e - 16^{***}$
	c	0.01818	0.005182	3.5083	0.0005063^{***}
	d	-0.8566	0.1688	-5.0756	$6.123e - 07^{***}$
Andrews weights	Coefficients	Estimate	Std. error	t value	p -value
	a	0.03020	0.005067	5.9611	$5.834e - 09^{***}$
	b	2.6548	0.2609	10.1765	$< 2.2e - 16^{***}$
	c	0.01818	0.007228	2.5152	0.012318^*
	d	-0.8566	0.3058	-2.8008	0.005365^{**}
Lumley weights	Coefficients	Estimate	Std. error	t value	p -value
	a	0.03020	0.005124	5.8949	$8.432e - 09^{***}$
	b	2.6548	0.2599	10.2142	$< 2.2e - 16^{***}$
	c	0.01818	0.007795	2.3322	0.020222^*
	d	-0.8566	0.3008	-2.8477	0.004649^{**}

Table 4: Regression results for the regression model (2.2)

break is indicated by $(c, d) \neq (0, 0)$. In particular, this shall be the case if we can check that $d \neq 0$, which may be done by simply computing a t -statistic. As there is again evidence of significant autocorrelation in the data as shown in the bottom right panel of Figure 2, we use heteroskedasticity- and autocorrelation-resistant testing here as well. Table 4 reports what is obtained using Andrews (1991) and Lumley and Heagerty (1999) weights, along with the results we would obtain if we did not account for the autocorrelation.

Results are similar for both correction methods: the hypothesis $d = 0$ is rejected at the 1% significance level and there is evidence of a structural break. It is noteworthy that the hypothesis $c = 0$ is also rejected, at the 5% level. More precisely, the intercept of model (2.1) actually increases after the financial crisis, while the slope b , representing the influence the EL has on the premium, decreases (as suggested by Table 3 and then confirmed by the fact that $d < 0$ in Table 4). Since, moreover, EL stayed broadly stable despite the financial crisis (see Table 1), this suggests that investors lost some of the trust they had in EL calculations after the financial crisis and appeared to favor a higher baseline price (represented by a) instead.

This loss of fitting power and related structural changes in the model at the time of the 2008 financial crisis are what motivated us to include the financial loss factor in our CAT bond pricing model. Let us now discuss the choice of financial risk measure we wish to use in this context.

Guided by regulation rules such as the Basel II and III Accords for banking regulation and the Solvency II Directive for insurance regulation, the Value-at-Risk (VaR) has been adopted by risk managers as an essential measure of risk, and is therefore one obvious candidate we could consider. Its formal definition is as follows: let X be a random variable with cumulative distribution function (cdf) G . The VaR of X at level $p \in (0, 1)$ is defined as

$$\text{VaR}_p(X) = G^{\leftarrow}(p) = \inf \{x : G(x) \geq p\}. \quad (2.3)$$

However, the VaR risk measure has been criticized in that it fails to measure tail losses when a tail event does occur; to put it differently, VaR only measures how high a loss must be so as to be qualified as extreme, but does not indicate how large such a loss typically is. By contrast, the CTE risk measure is the average of the worst $100(1 - p)\%$ of losses, which is defined as

$$\text{CTE}_p(X) = \frac{1}{1 - p} \int_p^1 \text{VaR}_q(X) dq,$$

provided that $E[X] < \infty$. Its name comes from the fact that when X is a continuous random variable, then $\text{CTE}_p(X) = E[X | X > \text{VaR}_p(X)]$, and as such CTE_p is exactly the average loss in the worst $100(1 - p)\%$ of cases. It is, therefore, a measure of what the practitioner should expect if an extreme loss with pre-defined probability actually occurs, which a single VaR cannot provide.

Moreover, VaR is not subadditive in general, and therefore does not define a coherent risk measure, contrary to CTE. Using the CTE risk measure thus allows the analyst to be flexible regarding how the risk variable is constructed: for instance, one interesting possibility would be to consider several stock market indices from different regions or some relevant assets, each acting as an individual risk, then compute their respective daily log-returns, and finally define the risk variable X by pooling these returns (*i.e.* averaging them over the number of indices/assets). This would give an idea of financial losses that can be either more global than that given by a single market index, or more localized if assets from a specific sector of the economy are chosen instead. In such a situation, the risk X is a sum of individual risks, and the subadditivity property becomes fully relevant. For the sake of simplicity, and since CAT bond premiums exhibit significant correlation with movements in the wider financial market, we choose here to work with a single risk variable constructed on the S&P 500 index, but there is nothing preventing an extension as we have described here.

The fact that CTE is a coherent measure of tail risk beyond the VaR is the main reason why the use of CTE instead of VaR is now being recommended by a significant part of the risk community, and not least by regulators in the Basel Committee on Banking Supervision (2013). Other, if more complicated, interesting coherent risk instruments are the classes of spectral risk measures and distortion risk measures (see *e.g.* Dowd and Blake, 2006) and, if one is willing to move away from quantile-based risk measures, the class of expectiles (see Newey and Powell, 1987; in an actuarial context, Kuan *et al.*, 2009). The CTE risk measure, however, has the advantages of simplicity and, crucially, straightforward interpretability, something that is arguably less apparent for expectiles.

Finally, and because our focus is to take tail risk into account, we do not consider central quantities such as the standard deviation, which do not capture the structure of tail risk and may even be undefined when the second moment of the loss variable does not exist. This is a distinct possibility since financial losses have empirically been shown to be heavy-tailed (see *e.g.* Gabaix *et al.*, 2003 as well as Chavez-Demoulin *et al.*, 2014). One alternative would have been to follow Dowd and Blake (2006) and select another coherent quantile-based risk measure, such as a spectral or distortion risk measure in order to assess tail risk. From the asymptotic point of view, such risk measures are linearly related to VaR when p is large (see Section 3.2 in El Methni and Stupfler,

2017a); that is, they can be scaled to the same value asymptotically as $p \rightarrow 1$. This makes the choice of the risk measure in our new model, introduced in (2.4) below, not essential for high p in the sense that we can always reach the same numerical evaluation of risk by tuning its regression coefficient. The well-behaved and simple CTE, that does not have the structural disadvantages of VaR, is therefore a natural choice for our work.

For the aforementioned reasons, we choose to work with the CTE risk measure in order to construct our financial loss variable. We are now ready to introduce the financial loss (FL) premium principle

$$\rho_{FL}(L) = a + b \text{EL} + c \text{CTE}_p(X), \quad (2.4)$$

for a , b and c all positive, where X represents the indicator of financial loss, which we take to be the negative daily log-return of S&P 500. A large positive value of X then represents the most dangerous situation in financial terms, while X negative can be considered as the profitable case. Let us also highlight that in the data set we consider for X , the values of the daily log-returns of S&P 500 were concentrated between -0.110 and 0.095 ; consequently, when there is a financial loss, namely X has taken positive values in the observation period and the confidence level p of CTE is high enough (*e.g.* above 50%), the value of $\text{CTE}_p(X)$ lies between 0 and 1 just as the value of EL does, and therefore the values of EL and $\text{CTE}_p(X)$ are comparable. In the following we show that the FL premium principle with 90% CTE, $\rho_{FL}(L) = a + b \text{EL} + c \text{CTE}_{0.90}(X)$, fits the post-crisis data better than the linear premium principle; we will also justify that the choice of the level $p = 0.9$, although providing the best fit, appeared to be largely inconsequential in terms of goodness-of-fit as long as one takes $p \geq 0.5$.

The empirical CTE is calculated based on one year of S&P 500 negative daily log-return data preceding the issue date of each CAT bond. More specifically, for any $p \in (0, 1)$,

$$\text{CTE}_p(X) \approx \frac{1}{\lfloor (1-p)n \rfloor} \sum_{i=\lfloor pn \rfloor}^n x_{[i]},$$

where $x_{[i]}$ is the i th largest negative daily log-return in n days (for a one-year period, $n \approx 260$). The ACF of the residuals of the fitted FL premium model are provided in Figure 3; they motivate again a correction for autocorrelation and heteroskedasticity. Numerical results, using such corrections, are reported in Table 5. It appears from these results that coefficient c , corresponding to $\text{CTE}_{0.90}$, is indeed highly significant and the adjusted R^2 markedly improves on that of the linear premium principle. This adjusted R^2 is essentially equivalent to that of the pre-crisis linear premium model, which seems to indicate that the FL model recovers a quantity of information equivalent to the one missing from the post-crisis implementation of the linear premium model. Interestingly, the coefficient b of EL in the FL premium model is only very slightly lower than in the post-crisis linear premium model, while the intercept a is much lower (half of what it was pre-crisis in the linear premium model, and a third of its value post-crisis). Our interpretation is that the perception of higher fixed risk loading in the post-crisis linear premium model was actually masking the fact that post-crisis premiums have been set in a significantly greater accordance with the behavior of the financial market compared to the pre-crisis period. Let us emphasize once more that our data does not seem to show that typical premium levels increased after the financial crisis, which is a different conclusion from that of Gurtler *et al.* (2016). This is because an increase in the intercept a of the linear premium or FL premium models does not necessarily translate into an increase of premium levels, as the occurrence of the latter also depends on other coefficients in the model as well as on EL and/or CTE levels. What our results do show, however, is that after the financial crisis, investors have been paying much more attention to market conditions and not merely to

Residuals, FL premium, post-crisis

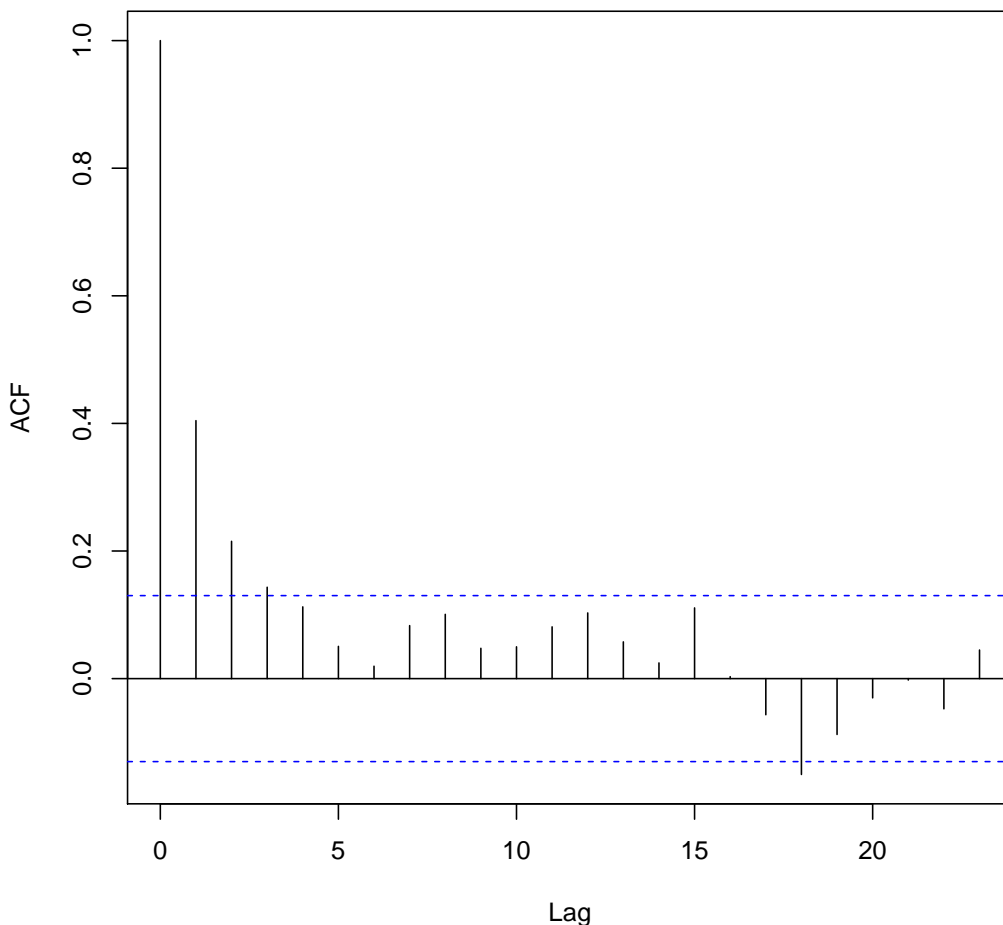


Figure 3: ACFs of the residuals, FL premium model $\rho(L) = a + bEL + cCTE_{0.90}(X)$.

EL calculations. Thus, the incorporation of a financial loss term results in a model that reflects investors' expectation on the return of CAT bond more accurately.

Now we justify that the FL premium with 90% CTE provides a (marginally) better fit than the FL premiums with other level of CTEs, but the choice of p is actually very flexible. Since, from the above, the FL premium principle is an improved model for the post-crisis data, we shall work with the 2008-2014 CAT bond data and compare the FL premium regression models (2.4) for $p \in \{50\%, 60\%, 70\%, 80\%, 90\%, 95\%\}$. We start at $p = 0.5$ because we primarily wish to evaluate the influence of financial tail risk on CAT bond pricing; furthermore, since the true value of $CTE_p(X)$ is unknown and estimated by the above empirical estimator, and noting that a year of S&P 500 daily log-returns data is made of roughly 260 observations, we cannot reasonably expect any such estimator to deliver reliable results if $p > 0.95$.

Our aim is to calculate the log-likelihood of each model and select the one with highest likelihood. To make sure that this procedure makes sense from the statistical point of view, we first check whether the errors in the regression model (2.4) can be considered Gaussian. Figure 4 shows Gaussian QQ-plots of the standardized residuals for all six models. It appears that in each case,

Coefficients	Estimate	Std. error	t value	p -value	Adj. R^2
a	0.015820	0.004092	3.866	0.000145***	0.7041
b	1.7329	0.08564	20.234	$< 2e - 16$ ***	
c	1.3802	0.1408	9.805	$< 2e - 16$ ***	

Table 5: Regression results for the FL premium principle (2.4) with $p = 90\%$ in the post-crisis market.

	CTE50	CTE60	CTE70	CTE80	CTE90	CTE95
Log-likelihood	542.3423	542.3758	542.219	542.5585	542.8444	542.5407
Adjusted R^2	0.6968	0.6981	0.6979	0.701	0.7041	0.7032

Table 6: Log-likelihoods for the regression models (2.4), where p varies in the set $\{50\%, 60\%, 70\%, 80\%, 90\%, 95\%\}$.

the left and central parts of the distribution of the standardized residuals are fitted very well by the standard Gaussian distribution and the right tail of the residuals looks a bit longer in each case, but only for 7 or 8 points. Since the post-crisis data set consists of 227 points, we consider this departure from normality reasonable for modeling purposes.

Because there is correlation in the residuals we need to account for this in the correlation structure of the errors in order to compute a correct log-likelihood for the model. To assess the correlation structure of the errors, we compute the ACF and partial autocorrelation function (PACF) of the residuals in all six cases, see Figures 5 and 6. In all six cases, the PACF cuts off after lag 1 and the ACF tails off. This suggests an autoregressive structure of order 1 (AR(1)) structure for the errors in these models.

We then compute the log-likelihood under an AR(1) model for the errors; results are summarized in Table 6. It is seen there that the log-likelihood is maximal for $p = 90\%$ among our six tested cases. We would therefore say that there is evidence that the 90% CTE model fits our data best. The values of adjusted R^2 are, however, all very close to and not less than 0.6968 when $p \geq 0.5$, meaning that in our opinion the choice of $p \geq 0.5$ is largely up to the practitioner and depends on the final objective of the modeling effort.

We conclude this section by providing some insight and recommendations regarding the choice of p . Let us first reiterate that an increasing risk aversion of market participants means that conservative investors are concerned about the potential impact of huge financial losses, and this is exactly the reason we propose to incorporate risk loading based on financial losses. Considering major financial losses, meanwhile, requires to consider the tail area of financial losses. This suggests to choose a high level p , but what such level should we consider? In current regulation frameworks, the level of VaR is set as 99% (Basel II) or 99.5% (Solvency II). Because VaR is criticized being not informative for tail risks, certain regulators have argued that CTE is a better risk measure and made recommendations for the confidence level p (e.g. 97.5%, see the Basel Committee on Banking Supervision, 2013, or 99%, see p.25 of McNeil *et al.*, 2015). One way to determine a level of CTE that can be used is to compute the value of p such that the value of the CTE equals that of VaR at 99%. This value of p depends of course on the underlying distribution of the risk. Many empirical studies have demonstrated the heavy-tailed character of log-returns on various stocks and stock indices and the tail indices are often found to lie between 1.5 and 3; see a summary of these findings in Ibragimov and Walden (2007). A quick calculation shows that for Pareto distributions with tail index ranging from 1.5 to 3, the level p required to make the CTE equal to

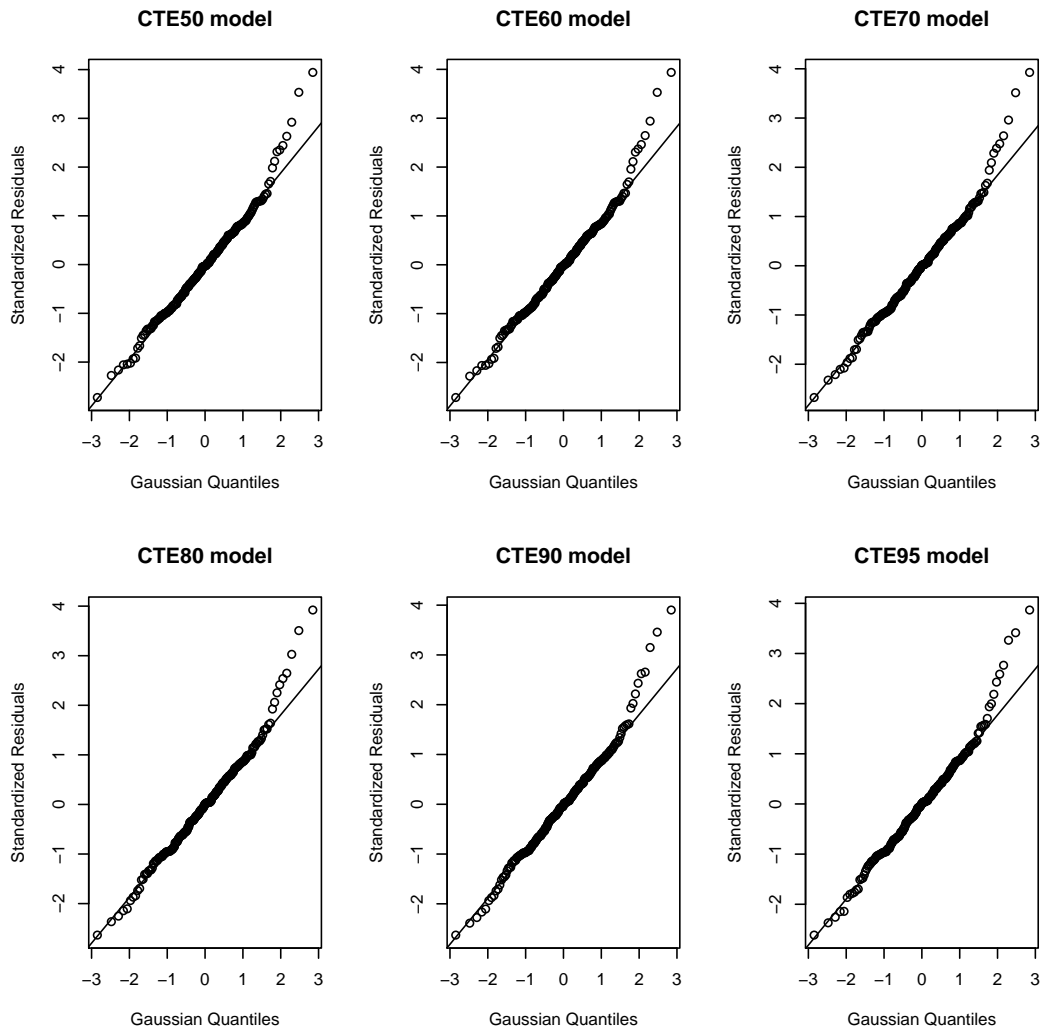


Figure 4: Gaussian QQ-plot of the standardized residuals for the regression model (2.4) with $p \in \{50\%, 60\%, 70\%, 80\%, 90\%, 95\%\}$.

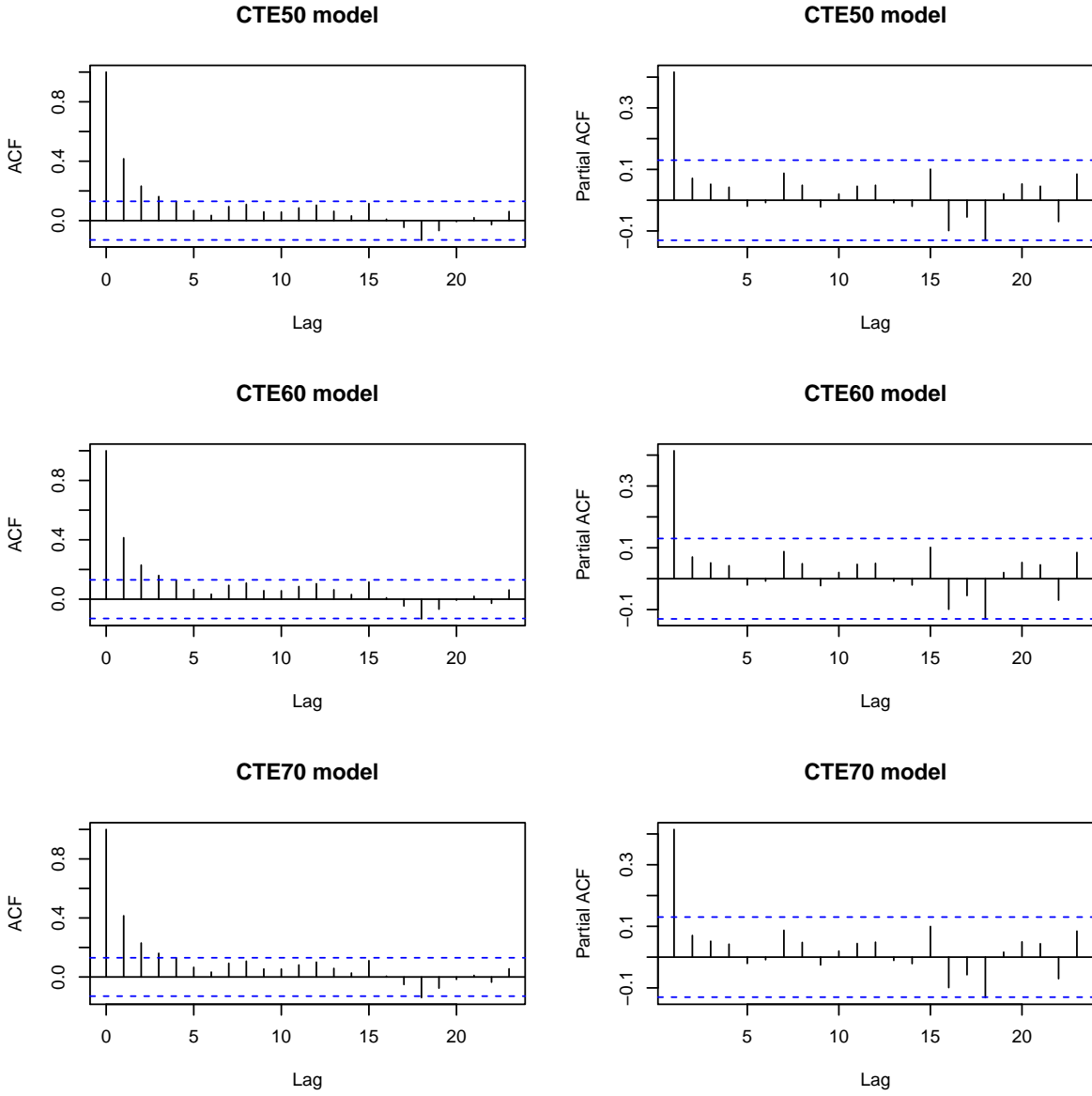


Figure 5: ACF (left panels) and PACF (right panels) for the regression model (2.4), case $p \in \{50\%, 60\%, 70\%\}$. First row: $p = 50\%$, second row: $p = 60\%$, third row: $p = 70\%$.

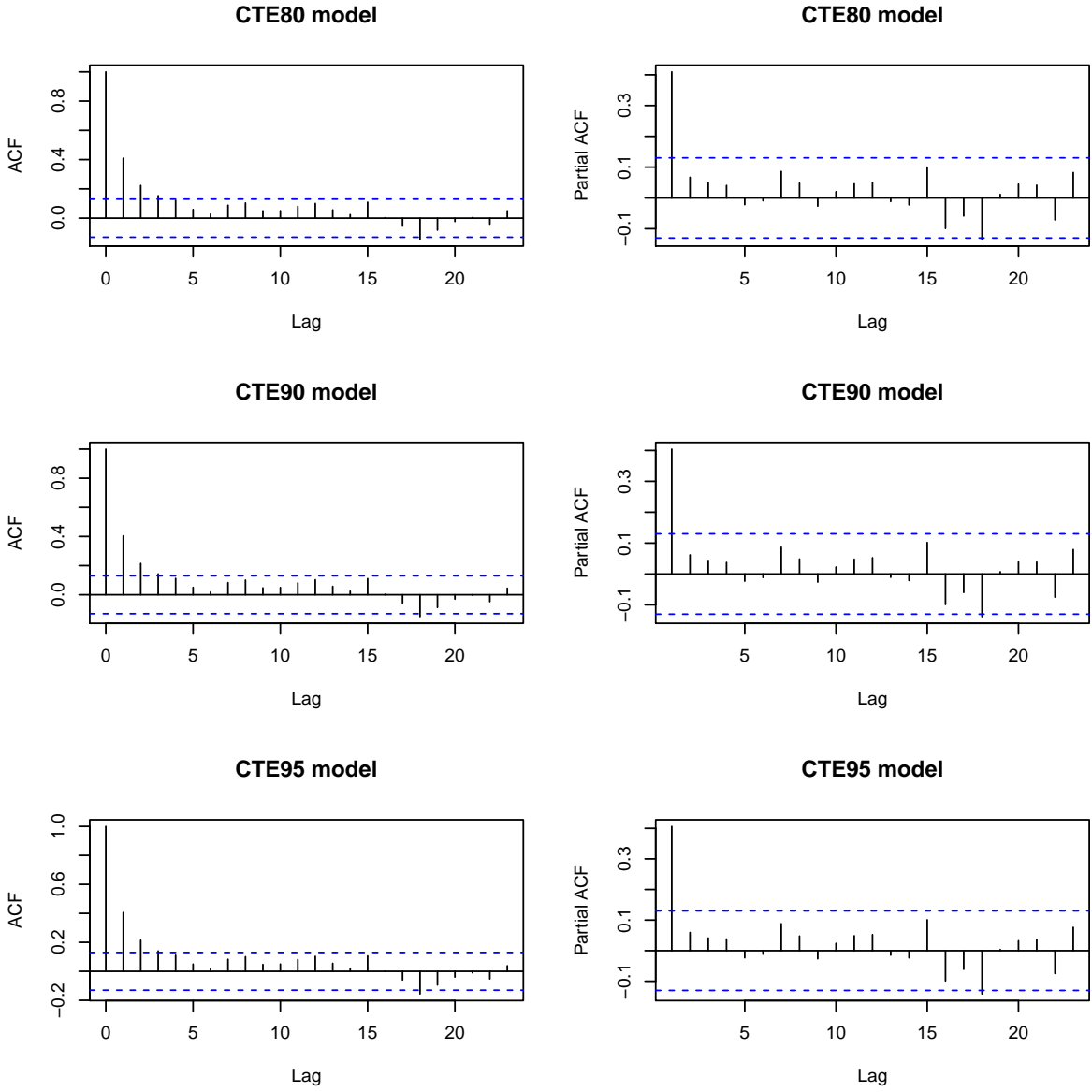


Figure 6: ACF (left panels) and PACF (right panels) for the regression model (2.4), case $p \in \{80\%, 90\%, 95\%\}$. First row: $p = 80\%$, second row: $p = 90\%$, third row: $p = 95\%$.

the 99% VaR is ranging from 95% to 97%. This is of course even higher if the recommended level of VaR is instead taken to be 99.5%, as the Solvency II regulatory framework recommends. On the one hand, and through this simple calculation, we can see why regulators, being inherently pessimistic, consider to propose to use the 99% level of CTE. On the other hand, regulatory criteria have been criticized by investors and financial firms precisely for being too pessimistic, and as such too costly to implement. Finally, and back to our context, the value of p to choose should depend on what we wish to model. In this application where we want to model the premium based on extreme behavior in the market, we would recommend using CTE at level 90% because it realizes a compromise between what the regulators recommend, what companies can comply with, and ease of estimation (including, as is the case here, when the sample size is in the hundreds). It also, we recall, provides a strong improvement in terms of goodness-of-fit upon the naive linear premium model in the post-crisis period.

3 Extreme value risk modeling

Catastrophe risk modeling is, by design, a key factor determining the premium of CAT bonds. Gurtler *et al.* (2016) argued though that their analysis of CAT bond data showed that “investors react with distrust of the expected loss calculated by catastrophe modeling companies”, suggesting that the modeling effort should be improved. We propose here to use methods from EVT, introduced in Section 3.1, to model catastrophic risks. Then, in Section 3.2, asymptotic analyses of the resulting predicted CAT bond premiums are carried out for any type of loss covered by a CAT bond, both in the linear premium and FL premium models.

3.1 The context of Extreme Value Theory

For the purpose of asymptotic analysis of CAT premiums, we briefly introduce the fundamental convergence result from EVT in this subsection.

A cdf F is said to belong to the MDA of a non-degenerate cdf H , denoted by $F \in \text{MDA}(H)$, if for an independent sample of size n from F , its properly linearly normalized maximum has a distribution converging weakly to H as $n \rightarrow \infty$. The classical Fisher-Tippett-Gnedenko theorem, attributed to Fisher and Tippett (1928) and Gnedenko (1943), states that up to location and scale, H has to be the GEV distribution whose standard version is given by

$$H_\gamma(t) = \exp \left\{ - (1 + \gamma t)^{-1/\gamma} \right\}, \quad \gamma \in \mathbb{R}, 1 + \gamma t > 0,$$

where the right-hand side is interpreted as $\exp \{-e^{-t}\}$ when $\gamma = 0$.

The regions $\gamma > 0$, $\gamma = 0$ and $\gamma < 0$ correspond to the so-called Frchet, Gumbel and Weibull domains of attraction, respectively. For a given distribution, belonging to such a domain of attraction is essentially a statement on the tail behavior of its survival function: the Frchet domain of attraction is the class of distributions whose survival function $\bar{F} = 1 - F$ decays roughly like a negative power of x , while belonging to the Gumbel domain of attraction means that the survival function has essentially an exponential decay near its right endpoint. Finally, a distribution which belongs to the Weibull domain of attraction must have a finite right endpoint x_F and its survival function then decays roughly like a positive power of $x - x_F$ near the endpoint.

It should be pointed out that, while a statement such as $F \in \text{MDA}(H)$ is in effect an assumption, it is the minimal assumption necessary to conduct a meaningful analysis of the extremes of a data set. Indeed, if the idea is to draw informative conclusions using the high values in the sample

of data, the minimum one can ask for is that a distributional convergence result about the highest value in the sample holds true.

3.2 Asymptotic analysis

In this subsection, we consider the asymptotic properties of CAT bond premiums as the attachment and exhaustion points get large. The analysis is valid for any type of trigger as long as we can justify that the catastrophic risk L follows an EVT model, no matter whether L represents the actual loss or a physical measure, the latter being the case we consider in our real data analysis. Suppose the term of the CAT bond can be divided into $N \geq 1$ periods such that in each period, the catastrophic risk can be quantified and (if $N > 1$) risks are mutually independent. We denote the catastrophic risk in the i th period by a nonnegative random variable L_i , for $1 \leq i \leq N$, with cdf $F(x) = 1 - \bar{F}(x) = \Pr(L \leq x)$ and upper endpoint $l^* \leq \infty$. The CAT bond is triggered by the maximum risk $M_N = \max\{L_1, \dots, L_N\}$ of the L_i over N periods; that is, if M_N exceeds the attachment point t , then the CAT bond starts to cover the loss. Since the L_i 's are independent and identically distributed random variables, the maximum M_N has cdf $F^N(x)$. The distribution of M_N may not be easy to approximate near its upper endpoint under no further hypothesis on F though. This is where EVT plays a crucial role: to get more information about the distribution of M_N , we assume that for all $1 \leq i \leq N$, $L_i \in \text{MDA}(H_\gamma)$ for some $\gamma \in \mathbb{R}$. Let us emphasize again that the domain of attraction $\text{MDA}(H_\gamma)$ includes a wide range of commonly used distributions which are suited to the capture of extreme risks. Moreover, and as we will show in Section 3 below, the particular parametric family of GP distributions constitutes a very convenient and versatile framework to model the excesses of the data above a high threshold.

Since a CAT bond covers the last layer of loss, our first main result focuses on the asymptotic behavior of the EL when the attachment and exhaustion points are at very high levels, that is, near l^* . In other words, we study the asymptotic behavior of

$$\text{EL} = \frac{\mathbb{E}[(M_N - t)_+] - \mathbb{E}[(M_N - h)_+]}{h - t}, \quad (3.1)$$

when t and h are approaching l^* . Intuitively, as the layer becomes higher, the EL should decrease. And indeed, the result in Theorem 3.1 below shows that, under some assumptions, the EL decreases proportionally with $\bar{F}(t)$. To make the presentation concise, all the proofs in this section are postponed to the Appendix.

Theorem 3.1 *Assume that $F \in \text{MDA}(H_\gamma)$ with $\gamma < 1$. Suppose further that both the exhaustion point t and the attachment point h are approaching l^* and are such that $\bar{F}(h)/\bar{F}(t)$ eventually converges to some positive constant λ . Then as $t \uparrow l^*$ the expected loss (3.1) is approximated by*

$$\text{EL} \sim \frac{N\lambda\gamma(\lambda^{\gamma-1} - 1)}{(1 - \lambda^\gamma)(1 - \gamma)} \bar{F}(t),$$

where the notation “ \sim ” means that the quotient of both sides tends to 1 as $t \uparrow l^*$.

Such an asymptotic expression can be used to illustrate how the layer affects the EL and the premiums. We show this by applying Theorem 3.1 to get the asymptotics for the linear premium principle (2.1).

Corollary 3.1 *Under the assumptions of Theorem 3.1, as $t \uparrow l^*$, the linear premium is approximated by*

$$\rho_{\text{linear}}(L) \approx a + \frac{bN\lambda\gamma(\lambda^{\gamma-1} - 1)}{(1 - \lambda^\gamma)(1 - \gamma)} \bar{F}(t). \quad (3.2)$$

Our last result considers the asymptotics of the FL premium principle. To obtain a result in the spirit of the previous corollary, we also consider the case when the level p in $\text{CTE}_p(X)$ approaches 1. And because this translates into considering the high quantiles of X only, we work in an extreme value framework dedicated to the considerations of high losses. Since much of the empirical evidence shows that the distribution of financial asset returns is heavy-tailed (see *e.g.*, Bradley and Taqqu, 2003, Resnick, 2007 and Chavez-Demoulin *et al.*, 2014), we assume that \bar{G} , the survival function of the financial losses, is regularly varying; that is, $\bar{G}(\cdot) \in \text{RV}_{-\beta}$, in the sense that

$$\lim_{t \rightarrow \infty} \frac{\bar{G}(tx)}{\bar{G}(t)} = x^{-\beta}, \quad x > 0.$$

This implies that $\bar{G}(x)$ behaves roughly like $x^{-\beta}$ in a neighborhood of infinity, and as such we assume that $\beta > 1$ in order to ensure the integrability of the quantile function of X and thus the existence of $\text{CTE}_p(X)$. We may now state the asymptotics of the FL premium principle assuming heavy-tailed financial losses.

Theorem 3.2 *Under the assumptions of Theorem 3.1, and as $t \uparrow l^*$, the FL premium principle (2.4) is approximated by*

$$\rho_{FL}(L) \approx a + \frac{bN\lambda\gamma(\lambda^{\gamma-1} - 1)}{(1 - \lambda\gamma)(1 - \gamma)}\bar{F}(t) + c\text{CTE}_p(X). \quad (3.3)$$

Furthermore, if the financial loss X has a survival function $\bar{G}(\cdot) \in \text{RV}_{-\beta}$ for some $\beta > 1$, then as $t \uparrow l^*$ and $p \uparrow 1$ we have

$$\rho_{FL}(L) \approx a + \frac{bN\lambda\gamma(\lambda^{\gamma-1} - 1)}{(1 - \lambda\gamma)(1 - \gamma)}\bar{F}(t) + \frac{c\beta}{\beta - 1}G^{\leftarrow}(p), \quad (3.4)$$

where G^{\leftarrow} denotes the quantile function related to G (see (2.3)).

Approximation (3.4) is of particular interest when the level p is chosen even higher than 90% (*i.e.* when the idea is to focus on the influence of the very highest losses on the premium) and/or when the size of the sample of data considered is small, although it should be recalled that the value of the coefficient c may depend on p since model (2.4) was originally stated for fixed p .

4 Application

In this section, we first introduce the POT method in EVT, which makes an efficient use of the data to fit the flexible parametric GP distribution to the high values in our sample. In Section 4.2, using this method, we fit a GP distribution to low precipitation data collected in Fort McMurray. Then, in Section 4.3, a wildfire CAT bond is proposed with precipitation as the trigger.

4.1 Peaks-Over-Threshold approach

The assumption that linearly normalized maxima converge in distribution is useful in theoretical derivations, for example to obtain the asymptotic expansions of the CAT bond premiums in Section 3.2. One simple way to use this condition in statistical applications is through the so-called *block maxima model*: the data is split into blocks of consecutive observations, whose sizes are so large that the Fisher-Tippett-Gnedenko theorem can be used to provide an approximation of the distribution of the maximum of the observations in each block. Although this technique can be shown to possess

interesting properties (for a nice recent account, see Ferreira and de Haan, 2015), it may be very wasteful of data since we only take one point, the maximum, in each block. In particular, if in a given block the second largest value is larger than all observations in the other blocks, this data point is discarded although it can legitimately be considered as part of the extremes of this sample.

In practice, the POT method, where all the data above some threshold (chosen by the analyst) can be used, is often applied instead. This technique considers all the data points above a high threshold, whose common distribution, called the excess distribution over threshold u , is defined as

$$F_u(x) = \Pr(X - u \leq x | X > u), \quad (4.1)$$

for $0 \leq x < x_F - u$, where x_F is the right endpoint of the distribution F . By the Pickands-Balkema-de Haan theorem (see *e.g.* Theorem 3.4.13(b) in Embrechts *et al.*, 1997), $F \in \text{MDA}(H_\gamma)$ if and only if there exists a positive function σ such that the excess distribution F_u can be approximated by a GP distribution $G_{\gamma, \sigma(u)}$ as the threshold u is approaching x_F , where

$$G_{\gamma, \sigma}(x) = 1 - (1 + \gamma x / \sigma)^{-1/\gamma}$$

is the cdf of the GP distribution; when $\gamma = 0$, the GP distribution $G_{\gamma, \sigma}(x)$ is understood as $1 - \exp(-x/\sigma)$. In other words, and provided a suitable high threshold u is chosen, the POT method allows one to retain all the data above the value u and regard it as (approximately) following a GP distribution. Such a technique, which we shall use in this work, allows one to have a comprehensive look at the extremes of a sample.

4.2 Analyzing the distribution of the Fort McMurray precipitation data

Wildfires have been a frequently occurring natural disaster during the summer months in North America. There are many factors that contribute to a wildfire, such as precipitation, temperature and wind speed. In this work, we consider the precipitation factor, especially focusing on the wildfires in Fort McMurray, Canada. Usually, dry fall and winter seasons along with a warm spring, which are considered as the consequences of the natural El Niño cycle, have high chances to cause a wildfire. Therefore, the amount of precipitation in three consecutive seasons is an important indicator of the likelihood of big wildfires during the following summer. We will show below with classical diagnostic plots in EVT how to model the distribution of precipitation.

The precipitation data set used in this work is obtained from the historical climate data provided on the website of the Government of Canada¹. It contains the monthly total precipitation (in millimeters) in Fort McMurray from September 1923 to May 2007. Since the fall, winter and spring seasons have a major impact on the occurrence of wildfires, we aggregate, for the N th year of data, the total monthly precipitation from September 1 in year N to May 31 in year $N + 1$. Usually a low amount of precipitation is a major reason behind the occurrence of wildfires, but the classical version of EVT we have introduced here deals with the right tail of a random variable, *i.e.* its high values. Hence, we simply transform the total of our nine months' precipitation into its reciprocal and then multiply it by 1000 to avoid too much rounding error in our computations. That is, if Y represents the total amount of precipitation from September to May in any two consecutive years, then the transformation

$$T(Y) = \frac{1000}{Y} = L \quad (4.2)$$

¹The website is <http://climate.weather.gc.ca/>

is the quantity used in our work as an indicator of wildfire risk. This gives us a total number of 83 data points L_i . Again, the data points generated this way come from a time series; while it is not clear that we are in the ideal situation when the data are independent, we point out that extreme value techniques have been shown to be resistant to autocorrelation and, more generally, violation of the independence assumption, at the price of more complicated and often wider confidence intervals; see *e.g.* Drees (2003). A crucial requirement for any extreme value technique to work, of course, is the validity of the MDA assumption, and we will then show first that it is reasonable to assume that the data can be modeled by a distribution belonging to $\text{MDA}(H_\gamma)$. For that purpose, the use of the POT approach, instead of the block maxima model, is especially justified with such a small data set.

The most important step in the POT method is to choose a proper threshold so that the GP distribution fits best the data beyond the threshold. If the threshold is chosen too low, the estimates are biased; if the threshold is too high, then too few exceedances remain which results in estimators having high variance. So far, the choice of such a threshold has been a widely debated topic (see the recent review paper by Scarrott and McDonald, 2012) but there is no universally-accepted, efficient approach, most situations requiring some kind of educated guess. We first conduct an exploratory analysis of the data to determine a suitable threshold and then use the Maximum Likelihood (ML) method to estimate the parameters.

A first, central question is to understand the type of tail behavior the data features. Although this is not necessary *per se* to estimate the parameters *via* the POT method, it will help us assess if our analysis gives plausible results. We start by drawing a QQ-plot of the empirical quantiles of the log-data versus theoretical quantiles of the standard exponential distribution whose cdf is $F_1(x) = 1 - \exp(-x)$. The rationale behind this is the following: a flat line at the right of the QQ-plot indicates that the data have a short-tailed distribution and thus may be modelled by a bounded distribution. We supplement this plot by drawing location-scale GEV QQ-plots of the data using the R function `fevd` contained in the R package `extRemes`. These plots are reported in Figure 7, where μ denotes location and σ denotes scale. All four plots suggest that the distribution should be described by a distribution with a negative shape parameter.

To get further insight into the right tail of the data, we draw a plot of the moment estimator of the extreme-value index γ of the data (Dekkers et al., 1989). Let $k + 1$ be the number of top order statistics taken into account for the estimation; the highest, second, ..., k th, $(k + 1)$ th order statistics are denoted by $L_{(n)}, L_{(n-1)}, \dots, L_{(n-k+1)}, L_{(n-k)}$ respectively. Let also

$$M_n^{(r)}(k) = \frac{1}{k} \sum_{i=0}^{k-1} (\log L_{(n-i)} - \log L_{(n-k)})^r, \quad r = 1, 2.$$

Then the moment estimator of γ is given by

$$\hat{\gamma}_{\text{Mom}}(k) = M_n^{(1)}(k) + 1 - \frac{1}{2} \left(1 - \frac{(M_n^{(1)}(k))^2}{M_n^{(2)}(k)} \right)^{-1}.$$

When the survival function of the modeling random variable L is further assumed to be second order regularly varying (see de Haan and Ferreira, 2006), it can be shown that $\hat{\gamma}_{\text{Mom}}(k)$ is asymptotically Gaussian for $k = k(n) \rightarrow \infty$ with $k/n \rightarrow 0$ and provided a bias condition holds, no matter what the value of γ is, contrary to what happens for the Hill estimator $M_n^{(1)}(k)$ (Hill, 1975), whose consistency requires that γ be positive. The pairs $(k, \hat{\gamma}_{\text{Mom}}(k))$ are represented on Figure 8. This

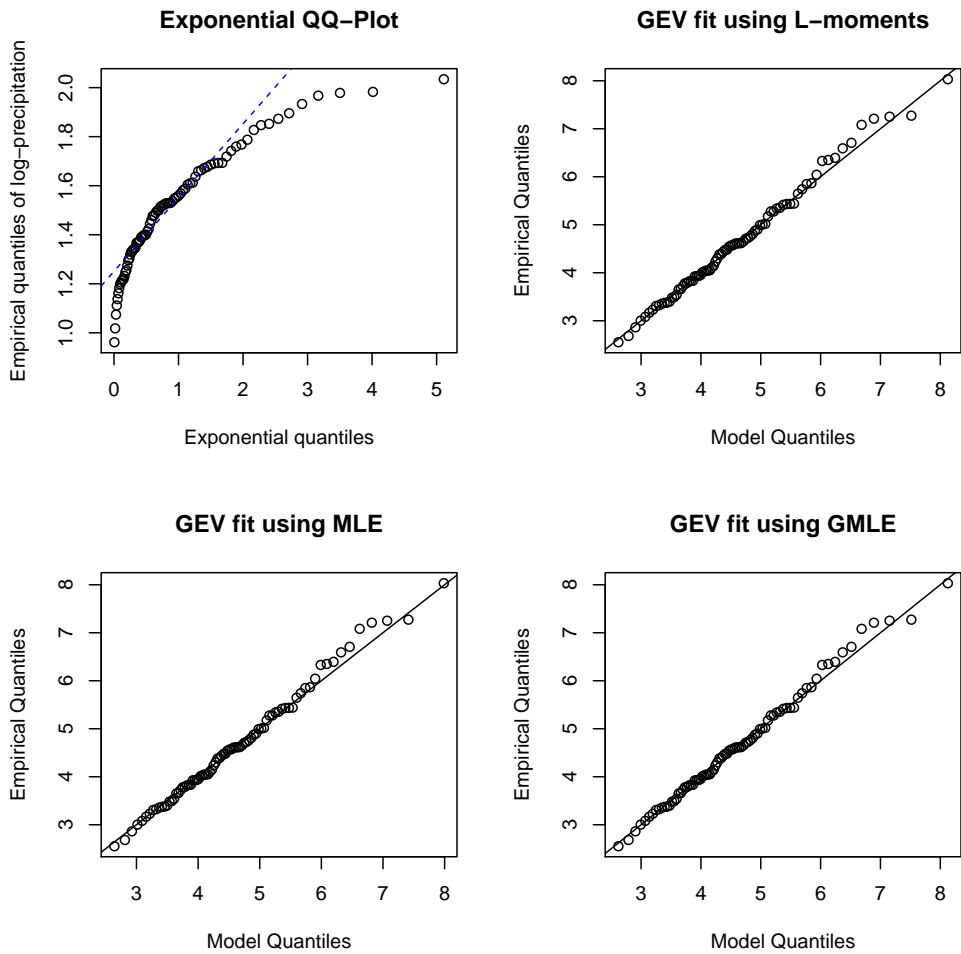


Figure 7: Top left: exponential QQ-plot of the log-precipitation data, top right: GEV QQ-plot of the precipitation data, estimates $(\hat{\mu}, \hat{\sigma}, \hat{\gamma}) = (4.084, 0.965, -0.025)$ given by an L-moments technique, bottom left: GEV QQ-plot of the precipitation data, estimates $(\hat{\mu}, \hat{\sigma}, \hat{\gamma}) = (4.096, 0.951, -0.036)$ given by the MLE, bottom right: GEV QQ-plot of the precipitation data, estimates $(\hat{\mu}, \hat{\sigma}, \hat{\gamma}) = (4.084, 0.965, -0.025)$ given by the GMLE.

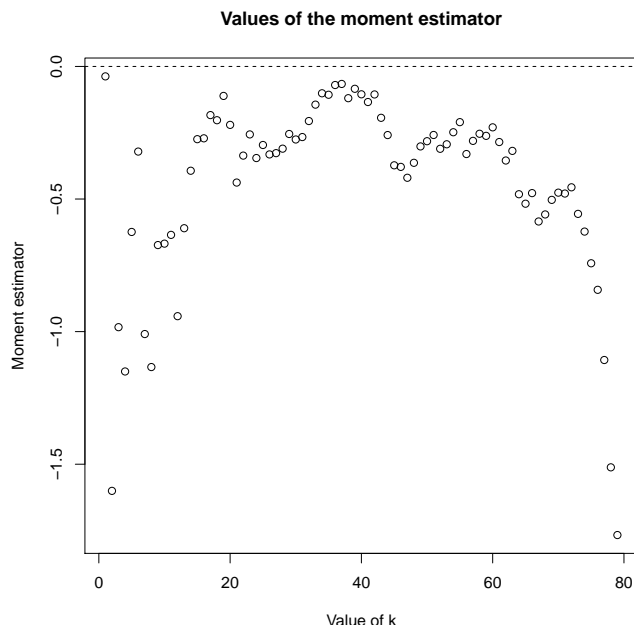


Figure 8: Plot of the moment estimates $\hat{\gamma}_{\text{Mom}}(k)$ as a function of k for the precipitation data.

plot largely confirms the previous conclusion: the data seems to give evidence of a short tail (*i.e.* negative shape parameter) or perhaps an exponentially decreasing tail (*i.e.* zero shape parameter).

Let us now work on the proper modeling of the extremes of the data using the POT approach. A commonly used device, as far as choosing the threshold is concerned, is the mean excess plot. The mean excess function of a random variable L is defined as

$$e(u) = \text{E}[L - u | L > u]. \quad (4.3)$$

It can be shown that if L follows a GP distribution with $\gamma < 1$, then $e(u)$ behaves linearly in u :

$$L \text{ is } G_{\gamma, \sigma} \text{ distributed} \Rightarrow e(u) = \frac{\sigma + \gamma u}{1 - \gamma}.$$

For more details, we refer the reader to Section 5.2 of McNeil *et al.* (2015) and Section 5.3.2 of Beirlant *et al.* (2004). A straightforward estimator of $e(u)$ based on (4.3) is given by

$$e_n(u) = \frac{\sum_{i=1}^n (L_i - u) 1_{\{L_i > u\}}}{\sum_{i=1}^n 1_{\{L_i > u\}}}. \quad (4.4)$$

If the data support the EVT assumption then it should be accurately modeled by a GP distribution over a high threshold and thus the plot of (4.4) as a function of u should become approximately linear for larger values of u . An upward trend indicates that the shape parameter γ is positive, a downward trend indicates that γ is negative and a roughly horizontal line indicates that γ is close to 0. The mean excess plot of the data, computed thanks to the function `mepplot` from the R package `evir`, is given in Figure 9. It looks from this plot that a good choice for the threshold u would be $u = 3.5$, after which the function e_n looks roughly linear indeed with a downward trend, thus supporting our first conclusions. This leaves us with 68 data points for the estimation. The corresponding QQ-plot of empirical quantiles of the data versus quantiles of the adjusted GP

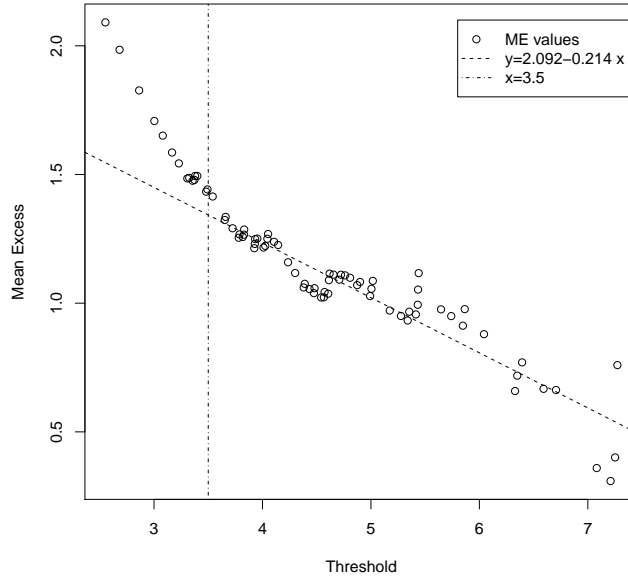


Figure 9: Mean excess plot of the precipitation data.

distribution using the ML estimator are given in Figure 10. The GP fit above $u = 3.5$ looks fairly good; the most extreme points in the data (above the value 7) seem to exhibit greater variability, although this is far from uncommon in extreme value models (see Ghosh and Resnick, 2010 and El Methni and Stupfler, 2017b). From this GP fit, the estimated scale $\hat{\sigma}$ is 1.990 and the estimated shape $\hat{\gamma}$ is -0.389 . The right endpoint is estimated to be

$$l^* = -\frac{\hat{\sigma}}{\hat{\gamma}} + u = 8.6125.$$

Namely, the lowest possible total precipitation over nine months is estimated to be 116.110 mm.

4.3 A wildfire bond

The 2016 Fort McMurray wildfire featured dry air mass, extremely high temperature and strong wind gust, according to the “Daily Data Report for May 2016” from Environment Canada². Low amounts of rainfall during the previous months were one of the major causes of exceptionally dry air and soil, and therefore contributed to this wildfire significantly. To mitigate extreme wildfire risk, we design a CAT bond for the wildfires in Fort McMurray. Due to the fact that the aggregated precipitation amount is an important indicator for the occurrence of wildfires, our suggested CAT bond has a parametric trigger related to precipitation.

To be more specific, first denote the total precipitation amount from September 1 in a given year to May 31 in the next year by Y . The quantity used to trigger the bond is the transformation $L = T(Y) = 1000/Y$ described in (4.2). We consider a nine-month bond which covers the months from September to May. The bond has a predetermined attachment point t and exhaustion point h . If the transformed precipitation L is below t then the bond is not triggered, with the entire

²The report can be accessed at http://climate.weather.gc.ca/climate_data/daily_data_e.html?StationID=27214&Year=2016&Month=5&Day=1

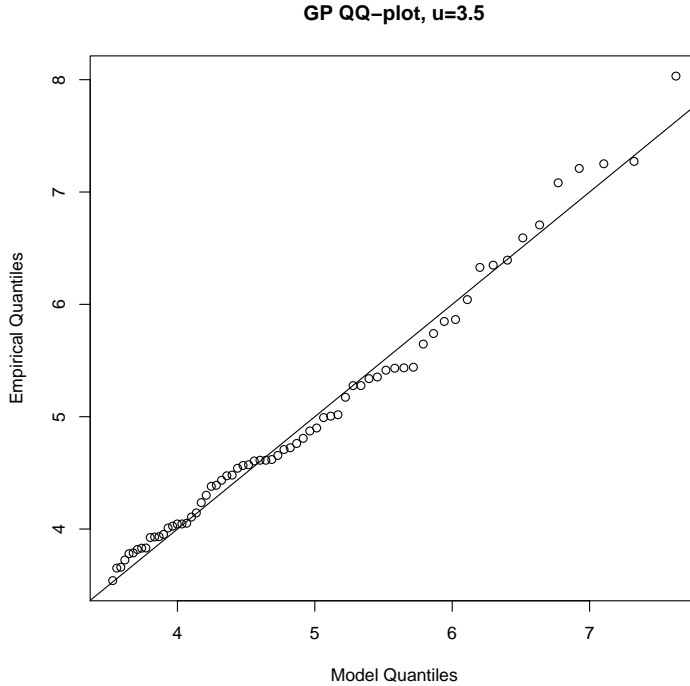


Figure 10: GP QQ-plot of the precipitation data above threshold $u = 3.5$. Estimated parameters $(\hat{\sigma}, \hat{\gamma}) = (1.990, -0.389)$ using the MLE.

principal paid back to the investor. If L is in between t and h , then the bond is triggered with a partial principal payment. If L is higher than h , then the bond is triggered with no principal paid back. We note that this type of bond lasts less than one year, but, if the data can be believed to be independent, it is straightforward to extend it to multiple years. Indeed, and with the notations of Section 3.2, an N -year bond would be triggered if the maximum $M_N = \max\{L_1, \dots, L_N\}$ of the transformed precipitation amounts L_1, \dots, L_N over the N -year term exceeds the attachment point t . If M_N exceeds the exhaustion point h , then the bond only covers the loss up to h . Again, we should point out here that, the data being weather time series data, the validity of the independence assumption is not clear, and therefore we consider it safer, from a statistical point of view, to restrict the bond to a nine-month period.

Next we illustrate how to utilize the results from the previous sections by discussing the choice of premium for this wildfire bond. Suppose a nine-month CAT bond on wildfire in Fort McMurray with precipitation as the parametric trigger is issued on September 1, 2015. As concluded in Section 2, we would recommend the use of the FL premium model with $p = 90\%$:

$$\rho_{FL}(L) = 0.015820 + 1.7329 \times EL + 1.3802 \times \text{CTE}_{0.90}, \quad (4.5)$$

where the coefficients are taken from our data analysis and specifically Table 5. The value of $\text{CTE}_{0.90}$ is calculated using S&P 500 data from September 1, 2014 to August 31, 2015. We also compare the results obtained using this model with the premiums calculated using the global, pre-crisis and post-crisis linear principle (2.1), with respective coefficients estimated in Section 2; see Table 3. In particular, the post-crisis linear premium model is

$$\rho_{\text{linear}}(L) = 0.04838 + 1.7982 \times EL. \quad (4.6)$$

Of course, at this modeling stage, the value of EL is unknown, but we may approximate it using a combination of Theorem 3.1 and our statistical analysis in Section 4.2. More precisely, by Theorem 3.2, the premium $\rho_{FL}(L)$ in (4.5) can be approximated by (3.3) when both t and h are large and $\bar{F}(h)/\bar{F}(t)$ is approximately equal to some constant λ ; similarly, the premium $\rho_{\text{linear}}(L)$ in (4.6) can be approximated by (3.2) in Corollary 3.1. In order to use these approximations, once the attachment point t is fixed, we need to calculate $\bar{F}(t)$ to apply our asymptotic relationships. Since the fitted excess distribution is the GP distribution, it is a consequence of (4.1) that for $x > u$, we can approximate the true survival probability by

$$\widehat{\bar{F}}(x) = \widehat{\pi}(u) \left(1 + \widehat{\gamma} \frac{x - u}{\widehat{\sigma}} \right)^{-1/\widehat{\gamma}}$$

where $\widehat{\pi}(u)$, the proportion of exceedances above level u in the data, is the straightforward empirical estimator of $\bar{F}(u)$. From Section 4.2, the estimated parameters are $\widehat{\sigma} = 1.9895$ and $\widehat{\gamma} = -0.3891$, and $\widehat{\pi}(u) = 68/83 = 0.8193$.

We consider an attachment point t ranging from 5 to 8.6125. By making the ratio λ vary in $\{0.1, 0.2, 0.3\}$, where $\lambda \approx \bar{F}(h)/\bar{F}(t)$ (or equivalently, by making h vary with t previously fixed), we can report calculated premiums in Figure 11. These premiums are in basis points (bps) and are calculated according to approximation (3.3). For a fixed probability of first loss (*i.e.* fixed attachment point t), a higher λ means a higher probability of exhaust (*i.e.* a lower exhaustion point h), which yields a higher premium: this is expected since a shorter layer leads to a higher likelihood of no payment to the investor at maturity. With the same ratio λ , as t increases, the premium decreases: again, this makes sense because a higher layer means a lower probability to have the bond triggered.

Next we consider what happens if this simple wildfire bond had indeed been issued on September 1, 2015. The total precipitation amount from September 2015 to May 2016 in Fort McMurray was 116.6 mm. With the transformation (4.2) we have $L = 8.5763$, which is very close to the estimated right endpoint of the precipitation distribution $l^* = 8.6125$. With such a high L , and although the definitive answer depends on the attachment and exhaustion points, the bond is very likely to be triggered. Then part or all of the principal will be not returned to the investor, and is instead kept by the (re)insurer to cover the huge claims caused by the wildfire. In Table 7, we summarize the contingent principal payment Z , which is the percentage of principal not returned to the investor, and the premium ρ for the bond, calculated in basis points according to the FL premium model and then to the global, pre-crisis and post-crisis linear premium models, with different attachment and exhaustion points linked by the ratio λ . It is clearly seen that when the coverage layer is very high, the principal is partially returned and the premium is low. In other cases when the coverage layer is lower, the bond is triggered without any part of the principal returned to investors (*i.e.* when $t = 6, 7$ for $\lambda = 0.1, 0.2$ and 0.3). It is also apparent that for a very high attachment point t , and within a given premium principle, the calculated premium is essentially a constant function of λ (and therefore of h). This is a consequence of the fact that for high t , the influence of EL becomes negligible due to it being asymptotically proportional to $\bar{F}(t)$; see Theorem 3.1.

From these last numerical results, it follows that the attachment and exhaustion points can therefore be fine-tuned to yield a CAT bond adapted to the particular purpose of sponsors. For instance in this example, if the goal is to only focus on extreme wildfire risk, then the coverage layer can be set high, close to the endpoint of the parametric trigger. This then yields a relatively low premium, which is attractive to the sponsor. At the same time and in this example, for the highest examined coverage layer, the FL premium principle returns a 32% higher premium than

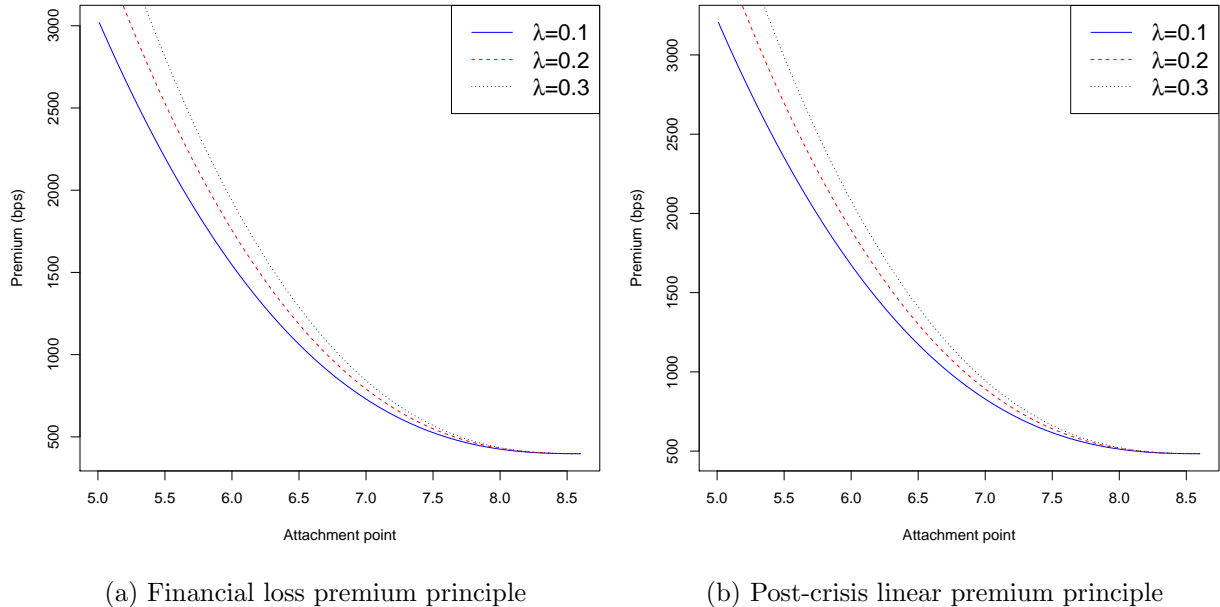


Figure 11: CAT bond modeling: the premium of the proposed one-year wildfire CAT bond, computed via the FL premium principle (4.5) and linear premium principle (4.6), as a function of the attachment point $t \in [5, l^*] = [5, 8.6125]$, for different values of the ratio $\lambda = \bar{F}(h)/\bar{F}(t)$. Blue solid line: $\lambda = 0.1$, red dashed line: $\lambda = 0.2$, black dotted line: $\lambda = 0.3$.

the pre-crisis linear premium model, and a 2% higher premium than the global linear premium model. By contrast, the FL premium is 18% lower than its post-crisis linear counterpart. This is, again, due to the post-crisis linear premium model predicting higher baseline premiums regardless of market behavior, while the FL premium principle reacts precisely to market movements. The difference between the premium predicted by the FL and global linear principles might appear insignificant; we would argue that this is simply due to the fact that in this precise example, the risk loads not due to EL in both the global linear model and FL premium model happened to be the same. If anything, this testifies of the reactivity of the FL principle when pricing high-attachment point CAT bonds: over the period considered here, the market did not experience any unusual shocks, and as such we would not necessarily expect a strong departure from price calculations under “stationary regime” computations. By contrast, if the period considered had featured extreme market movements, then this would have been reflected in the calculation of the premium by the FL principle, but the linear premium model would not have captured this. It is also interesting to note that for lower (but still high) attachment points, the FL principle yields the lowest premium among the four principles tested here. This is because the EL coefficient b is, among all four models, the lowest in the FL principle; besides, in such cases, the premium is strongly driven by the EL (since $\bar{F}(t)$ is still relatively high) and therefore, the higher the coefficient b in such a model, the higher the premium. The FL principle, which diverts the focus from EL calculations to market conditions, appears therefore to be a liberal pricing principle in standard cases, while it defines a conservative, but not overly pessimistic, prediction rule if the focus is on the most extreme events.

These results also carry practical consequences. Our results show that if the focus is to (re)insure the most extreme events (*i.e.* if a very high t is considered) then CAT bond investors

λ	t	h	Z	ρ_{FL}	ρ_{linear} (global)	ρ_{linear} (pre-crisis)	ρ_{linear} (post-crisis)
0.1	6	7.55	100%	1545.89	1884.11	2061.004	1675.24
	7	7.95	100%	729.99	822.39	811.06	828.60
	8.56	8.5911	43.76%	397.75	390.07	302.08	483.85
0.2	6	7.22	100%	1757.06	2158.89	2384.51	1894.36
	7	7.75	100%	791.10	901.92	904.68	892.02
	8.56	8.5844	55.65%	397.76	390.08	302.09	483.86
0.3	6	6.98	100%	1935.92	2391.65	2658.53	2079.97
	7	7.60	100%	842.86	969.28	983.98	945.73
	8.56	8.5796	69.24%	397.77	390.09	302.10	483.87

Table 7: The contingent principal payment and the premium of the wildfire bond with various attachment and exhaustion points.

will tend to get at least a significant part of their investment back, and we may estimate this proportion using our extreme value framework. The premium in this case is of course lower than if the coverage layer was set at a lower level, but certain risk-averse investors may still be attracted by this kind of financial products. (Re)insurers, meanwhile, should expect lower prices when the market is going well, and higher premiums when the market is on a downward trend. This is intuitive, since investors will understandably find it riskier to invest when the market is volatile, and will therefore require higher yields before investing. The fact that the value of the premium predicted by the FL principle is conservative but not unreasonably pessimistic, and most importantly more reactive to market behavior than standard solutions, should come as an important step towards the generalization of CAT bonds for risk diversification purposes. Let us finally conclude this data analysis by pointing out again that the trigger used in the bond is actually determined based on information available before the wildfire season. The bond can thus be triggered before the real disaster, which may serve as a warning system for (re)insurers to gather enough capital so as to be prepared for potential claims. It is, therefore, our opinion that the present analysis shows how CAT bonds can be specifically designed to diversify extreme (wildfire) risk to the capital market, and simultaneously help (re)insurers to deal with the largest claims preventively, using adapted extreme value tools. Part of our future research will be to refine the trigger: for instance, if more relevant information, such as temperature and wind speed, is incorporated, a combined trigger can then be expected to better indicate the possibility of a big wildfire.

5 Conclusion

By examining the pre- and post-crisis financial market, we show with an empirical study that financial losses are positively correlated with CAT bond premiums, and we see an increase in estimated correlation levels. A main justification for this is the increase in risk aversion of market participants after the crisis. We also find evidence of a breakpoint in the linear premium model, happening at the time of the financial crisis. In particular, the post-crisis linear premium model points to an increase in the fixed level of risk load and a decrease in the coefficient of EL, but we also find that this model does not explain the post-crisis CAT bond market as well as it did before the crisis. We then propose a FL premium principle for CAT bonds, which uses the risk measure CTE to measure financial losses. We find that, in the post-crisis period, this new premium principle recovers a quantity of information equivalent to the one lost by the linear premium model after the financial crisis. This indicates that in the post-crisis market, the burden of modeling the

increase in risk aversion levels of investors should be shared between the fixed risk load and a separate financial loss factor, instead of just universally increasing the level of the fixed risk load. A further consequence is that, according to the FL premium principle, one should expect lower CAT bond premiums when the financial market is going well, and higher premiums when the market is on a downward trend. This new premium principle is also shown to be flexible with respect to the confidence/exceedance level of CTE. Our recommendation would be to use the 90% level, which seems to be a good compromise between the regulators' goals, the companies' need to stay competitive and accuracy of estimation.

Next, by using tools from EVT, we are able to obtain asymptotic expansions of the FL premium. Such approximations, who illustrate how a premium calculated via the FL principle reacts to changes in the position and width of the coverage layer as well as to how long the CAT bond's term is and the tail behavior of the triggering risk variable, provide a significant amount of information during the design stage of a CAT bond. This is then applied to the design of a nine-month CAT bond for wildfire risk in Fort McMurray: we define the triggering variable as the (suitably transformed) total amount of precipitation data recorded during the nine months preceding the summer season, and we fit a GP distribution to the right tail of this random variable using the POT method. The advantage of designing a CAT bond in this way is that, as the amount of precipitation is an effective indicator of wildfires, (re)insurance companies can get prepared before a potential disaster once the bond is triggered, and this clearly helps (re)insurers share the risk with the capital market. We further illustrate how different pricing models compare on this situation to complement the conclusions reached in our empirical CAT bond study.

6 Appendix

The concept of extended regular variation (ERV) is useful for our unified derivation. By definition, a positive measurable function $f(\cdot)$ is said to be extended regularly varying at $+\infty$ with index $\gamma \in \mathbb{R}$, denoted by $f(\cdot) \in \text{ERV}_\gamma$, if there is an auxiliary function $a(\cdot) > 0$ such that, for all $s > 0$,

$$\lim_{t \rightarrow \infty} \frac{f(st) - f(t)}{a(t)} = \frac{s^\gamma - 1}{\gamma}, \quad (6.1)$$

where the right-hand side is interpreted as $\log s$ when $\gamma = 0$. The auxiliary function $a(\cdot)$ can be chosen to be

$$a(t) = \begin{cases} \gamma f(t), & \gamma > 0, \\ f(t) - t^{-1} \int_0^t f(u) du, & \gamma = 0, \\ -\gamma(f(\infty) - f(t)), & \gamma < 0. \end{cases} \quad (6.2)$$

Note that, for $\gamma = 0$, as $t \rightarrow \infty$, we have $a(t) = o(f(t))$ provided $f(\infty) = \infty$, while $a(t) = o(f(\infty) - f(t))$ provided $f(\infty) < \infty$. See Appendix B of de Haan and Ferreira (2006) for more discussions on extended regular variation.

The MDA of the GEV distribution is related to ERV through the so-called tail quantile function

$$U(x) = \left(\frac{1}{F} \right)^{\leftarrow} (x) = F^{\leftarrow} \left(1 - \frac{1}{x} \right), \quad x > 1. \quad (6.3)$$

We recall that in (6.3), F^{\leftarrow} denotes the left-continuous inverse of the nondecreasing function F , that is

$$F^{\leftarrow}(z) = \inf\{t \in \mathbb{R} \mid F(t) \geq z\}.$$

We have $F \in \text{MDA}(H_\gamma)$ if and only if $U(\cdot) \in \text{ERV}_\gamma$ with the auxiliary function $a(\cdot)$ given in (6.2) in terms of $U(\cdot)$; see Theorem 1.1.6 of de Haan and Ferreira (2006).

The following lemma is a restatement of Theorem B.2.18 of de Haan and Ferreira (2006), originally attributed to Drees (1998):

Lemma 6.1 *Let $f(\cdot) \in \text{ERV}_\gamma$ for $\gamma \in \mathbb{R}$, namely, relation (6.1) holds for all $s > 0$ and for an auxiliary function $a(\cdot)$ given in (6.2). Then for every small $\varepsilon, \delta > 0$, there is $t_0 = t_0(\varepsilon, \delta) > 0$ such that for all s, t with $t > t_0, st > t_0$, we have*

$$\left| \frac{f(st) - f(t)}{a(t)} - \frac{s^\gamma - 1}{\gamma} \right| \leq \varepsilon \max(s^{\gamma+\delta}, s^{\gamma-\delta}). \quad (6.4)$$

Taking the supremum of both sides of the inequality (6.4) with respect to s over a closed positive interval containing 1, and then letting the interval boil down to the point 1, we can easily prove that

$$\lim_{t \rightarrow \infty} \frac{f(t \pm 0) - f(t)}{a(t)} = 0$$

where $f(t + 0)$ (resp. $f(t - 0)$) denotes the left (resp. right) limit of f at t , when it exists. It follows from this and (6.1) that, for all $s > 0$,

$$\lim_{t \rightarrow \infty} \frac{f(st) - f(t \pm 0)}{a(t)} = \frac{s^\gamma - 1}{\gamma}. \quad (6.5)$$

Since L_1, \dots, L_N are independent and identically distributed random variables with common cdf F , the cdf of the maximum $M_N = \max\{L_1, \dots, L_N\}$ is $\Pr(M_N \leq x) = F^N(x)$. For any cdf F , we have the following general result: as $x \rightarrow \infty$,

$$\begin{aligned} \Pr(M_N > x) &= 1 - F^N(x) \\ &= (1 - F(x))(1 + F(x) + F^2(x) + \dots + F^{N-1}(x)) \\ &\sim N\bar{F}(x). \end{aligned} \quad (6.6)$$

This provides a simple connection between the L_i and M_N .

Proof of Theorem 3.1. Notice that as $t \rightarrow l^*$,

$$\begin{aligned} \mathbb{E}[(M_N - t)_+] &= \int_t^{l^*} (z - t) dF^N(z) \\ &= \int_0^{l^*-t} [1 - F^N(z + t)] dz \\ &\sim N \int_0^{l^*-t} \bar{F}(z + t) dz = N\mathbb{E}[(L - t)_+], \end{aligned}$$

where the penultimate step is due to (6.6) together with the dominated convergence theorem since $\gamma < 1$. This relation allows us to focus on $\mathbb{E}[(L - t)_+]$.

Note now that the survival function $\bar{F}(t)$ is, in a left-neighborhood of its right endpoint l^* , equivalent to a twice continuously differentiable and decreasing function $\bar{F}_0(t)$ (see Remark 1.2.8 in de Haan and Ferreira, 2006) having the same endpoint l^* and the same regular variation properties. As such, if the attachment point $t \rightarrow l^*$, we have $x = 1/\bar{F}(t) \rightarrow \infty$. Recall further the function $U(\cdot)$ defined in (6.3) and let V be a random variable uniformly distributed on $(0, 1)$. It is easy to verify that L conditional on $L > t$ is equal in distribution to $U(x/V)$; namely,

$$L | (L > t) \stackrel{d}{=} U(x/V).$$

Hence,

$$\begin{aligned} \mathbf{E} [(L - t)_+] &= \frac{1}{x} \mathbf{E} [L - t | L > t] = \frac{1}{x} \mathbf{E} [U(x/V) - t] \\ &= \frac{1}{x} \int_0^1 [U(x/v) - t] dv. \end{aligned}$$

We then have

$$\frac{x \mathbf{E} [(L - t)_+]}{a(x)} \leq \int_0^1 \frac{U(x/v) - U(x)}{a(x)} dv.$$

Recall that $F \in \text{MDA}(H_\gamma)$ if and only if $U(\cdot) \in \text{ERV}_\gamma$. It follows from Lemma 6.1 that the integrand in the right-hand side is such that

$$\begin{aligned} \left| \frac{U(x/v) - U(x)}{a(x)} \right| &\leq \left| \frac{U(x/v) - U(x)}{a(x)} - \frac{v^{-\gamma} - 1}{\gamma} \right| + \frac{v^{-\gamma} - 1}{\gamma} \\ &\leq v^{-(\gamma+1)/2} + \frac{v^{-\gamma} - 1}{\gamma} \end{aligned}$$

for x large enough. The dominating function is integrable on $(0, 1)$ because $\gamma < 1$ (when $\gamma = 0$, the second part is $\log(1/v)$ which is integrable as well). An application of the dominated convergence theorem then yields that, as $t \rightarrow l^*$,

$$\lim_{t \uparrow l^*} \frac{x \mathbf{E} [(L - t)_+]}{a(x)} = \lim_{x \rightarrow \infty} \int_0^1 \frac{U(x/v) - U(x)}{a(x)} dv = \int_0^1 \frac{v^{-\gamma} - 1}{\gamma} dv.$$

Then when $x/y = \bar{F}(h)/\bar{F}(t) \rightarrow \lambda$, we have thanks to (6.5) and the inequalities

$$U(x) \leq t \leq U(x+0), \quad U(y) \leq h \leq U(y+0)$$

that

$$\frac{\mathbf{E} [(L - t)_+]}{h - t} \sim \frac{a(x) \int_0^1 \frac{v^{-\gamma} - 1}{\gamma} dv}{x (U(y) - U(x))} \sim \frac{1}{x} \frac{\gamma}{\lambda^{-\gamma} - 1} \int_0^1 \frac{v^{-\gamma} - 1}{\gamma} dv.$$

Similarly we have

$$\frac{\mathbf{E} [(L - h)_+]}{h - t} \sim \frac{a(y) \int_0^1 \frac{v^{-\gamma} - 1}{\gamma} dv}{y (U(y) - U(x))} \sim \frac{1}{y} \frac{-\gamma}{\lambda^\gamma - 1} \int_0^1 \frac{v^{-\gamma} - 1}{\gamma} dv.$$

Therefore, since again $x/y = \bar{F}(h)/\bar{F}(t) \rightarrow \lambda$,

$$\text{EL} \sim \frac{N \lambda \gamma (\lambda^{\gamma-1} - 1)}{(1 - \lambda^\gamma)(1 - \gamma)} \bar{F}(t).$$

This ends the proof. \square

Proof of Theorem 3.2. We only need to focus on the asymptotic expansion of $\text{CTE}_p(X)$ as $p \rightarrow 1$, which, however, is well known in the literature. Here we present the proof for completeness.

Since $\overline{G}(\cdot) \in \text{RV}_{-\beta}$, we have that $G^{\leftarrow}(1 - \cdot) \in \text{RV}_{-1/\beta}(+0)$. Note that

$$\begin{aligned} \frac{1}{1-p} \int_p^1 G^{\leftarrow}(q) dq &= \frac{1}{1-p} \int_p^1 G^{\leftarrow}(1 - (1-q)) dq \\ &= \frac{G^{\leftarrow}(p)}{1-p} \int_p^1 \frac{G^{\leftarrow}(1 - (1-q))}{G^{\leftarrow}(1 - (1-p))} dq \\ &\sim \frac{G^{\leftarrow}(p)}{1-p} \int_p^1 \left(\frac{1-q}{1-p} \right)^{-1/\beta} dq \\ &= \frac{\beta}{\beta-1} G^{\leftarrow}(p), \end{aligned}$$

where the third step is due to the uniform convergence properties of $\text{RV}_{-1/\beta}(+0)$ functions. This ends the proof. \square

Acknowledgments. The authors would like to thank two anonymous referees for their constructive and helpful remarks which resulted in significant improvements to this paper. Support for Fan Yang from grant from the Natural Sciences and Engineering Research Council of Canada (grant number 04242) is gratefully acknowledged.

References

- [1] Alvarado, E., Sandberg, D.V. and Pickford, S.G. (1998). Modeling large forest fires as extreme events. *Northwest Science*, **72**, 66–75.
- [2] Andrews, D.W.K. (1991). Heteroskedasticity and autocorrelation consistent covariance matrix estimation. *Econometrica*, **59**, 817–858.
- [3] Basel Committee on Banking Supervision (2013). *Fundamental review of the trading book: A revised market risk framework*. Basel: Bank for International Settlements.
- [4] Beirlant, J., Goegebeur, Y., Segers, J. and Teugels, J. (2004). *Statistics of Extremes: Theory and Applications*. John Wiley & Sons.
- [5] Beirlant, J., Vynckier, P. and Teugels, J. L. (1996). Excess functions and estimation of the extreme value index. *Bernoulli*, **2**(4), 293–318.
- [6] Bradley, B.O. and Taqqu, M.S. (2003). Financial risk and heavy tails. In Rachev, S.T. (ed.), *Handbook of Heavy-Tailed Distributions in Finance*, Elsevier, Amsterdam, 35–103.
- [7] Braun, A. (2016). Pricing in the Primary Market for CAT Bonds: New Empirical Evidence. *Journal of Risk and Insurance*, **83**(4), 811–847.
- [8] Bühlmann, H. (1970). *Mathematical Models in Risk Theory*. Springer-Verlag.
- [9] Carayannopoulos, P. and Perez, M.F. (2015). Diversification through Catastrophe Bonds: Lessons from the Subprime Financial Crisis. *The Geneva Papers on Risk and Insurance-Issues and Practice*, **40**(1), 1–28.

- [10] Chavez-Demoulin, V., Embrechts, P. and Sardy, S. (2014). Extreme-quantile tracking for financial time series. *Journal of Econometrics*, **181**, 44–52.
- [11] Cummins, J.D. and Weiss, M. A. (2009). Convergence of Insurance and Financial Markets: Hybrid and Securitized Risk-Transfer Solutions. *Journal of Risk and Insurance*, **76**(3), 493–545.
- [12] Dekkers, A.L.M., Einmahl, J.H.J. and de Haan, L. (1989). A moment estimator for the index of an extreme-value distribution. *Annals of Statistics*, **17**, 1833–1855.
- [13] de Haan, L. and Ferreira, A. (2006). *Extreme Value Theory: an Introduction*. Springer, New York.
- [14] Dowd, K. and Blake, D. (2006). After VaR: the theory, estimation, and insurance applications of quantile-based risk measures. *Journal of Risk and Insurance*, **73**(2), 193–229.
- [15] Drees, H. (1998). On smooth statistical tail functionals. *Scandinavian Journal of Statistics*, **25**, 187–210.
- [16] Drees, H. (2003). Extreme quantile estimation for dependent data, with applications to finance. *Bernoulli*, **9**, 617–657.
- [17] El Methni, J. and Stupfler, G. (2017a). Extreme versions of Wang risk measures and their estimation for heavy-tailed distributions. *Statistica Sinica*, **27**(2), 907–930.
- [18] El Methni, J. and Stupfler, G. (2017b). Improved estimators of extreme Wang distortion risk measures for very heavy-tailed distributions. To appear in *Econometrics and Statistics*.
- [19] Embrechts, P., Klüppelberg, C. and Mikosch, T. (1997). *Modelling extremal events for insurance and finance*. Springer-Verlag, Berlin.
- [20] Ferreira, A. and de Haan, L. (2015). On the block maxima method in extreme value theory: PWM estimators. *Annals of Statistics*, **43**(1), 276–298.
- [21] Fisher, R.A. and Tippett, L.H.C. (1928). Limiting forms of the frequency distribution of the largest or smallest member of a sample. *Mathematical Proceedings of the Cambridge Philosophical Society*, **24**(2), 180–190.
- [22] Froot, K.A. (2001). The market for catastrophe risk: a clinical examination. *Journal of Financial Economics*, **60**(2), 529–571.
- [23] Gabaix, X., Gopikrishnan, P., Plerou, V. and Stanley, H.E. (2003). A theory of power-law distributions in financial market fluctuations. *Nature*, **423**(6937), 267–270.
- [24] Galeotti, M., Gürtler, M. and Winkelvos, C. (2013). Accuracy of premium calculation models for CAT bonds—an empirical analysis. *Journal of Risk and Insurance*, **80**(2), 401–421.
- [25] Ghosh, S. and Resnick, S. (2010). A discussion on mean excess plots. *Stochastic Processes and their Applications*, **120**(8), 1492–1517.

- [26] Gnedenko, B.V. (1943). Sur la distribution limite du terme maximum d’une série aléatoire. *Annals of Mathematics*, **44**(3), 423–453.
- [27] Görtler, M., Hibbeln, M. and Winkelvos, C. (2016). The impact of the financial crisis and natural catastrophes on CAT bonds. *Journal of Risk and Insurance*, **83**, 579–612.
- [28] Hill, B.M. (1975). A simple general approach to inference about the tail of a distribution. *Annals of Statistics*, **3**, 1163–1174.
- [29] Hoeppe, P. (2016). Trends in weather related disasters – Consequences for insurers and society. *Weather and Climate Extremes*, **11**, 70–79.
- [30] Ibragimov, R. and Walden, J. (2007). The limits of diversification when losses may be large. *Journal of Banking & Finance*, **31**(8), 2551–2569.
- [31] Koutsoyiannis, D. (2004). Statistics of extremes and estimation of extreme rainfall: II. Empirical investigation of long rainfall records. *Hydrological Sciences Journal*, **49**(4), 591–610.
- [32] Kuan, C.-M., Yeh, J.-H. and Hsu, Y.-C. (2009). Assessing value at risk with CARE, the Conditional Autoregressive Expectile models. *Journal of Econometrics*, **2**, 261–270.
- [33] Lane, M.N. (2000). Pricing Risk Transfer Transactions. *ASTIN Bulletin*, **30**(2), 259–293.
- [34] Lane, M. and Mahul, O. (2008). Catastrophe risk pricing: an empirical analysis. *World Bank Policy Research Working Paper Series*.
- [35] Lumley, T. and Heagerty, P. (1999). Weighted empirical adaptive variance estimators for correlated data regression. *Journal of the Royal Statistical Society: Series B*, **61**, 459–477.
- [36] Major, J.A. and Kreps, R.E. (2002). Catastrophe Risk Pricing in the Traditional Market. In Lane, M. (ed.), *Alternative Risk Strategies*, London, 201–222.
- [37] McNeil, A.J., Frey, R. and Embrechts, P. (2015). *Quantitative Risk Management: Concepts, Techniques, and Tools*. Princeton University Press.
- [38] McNeil, A. J. and Saladin, T. (1997). The peaks over thresholds method for estimating high quantiles of loss distributions. In *Proceedings of 28th International ASTIN Colloquium*, 23–43.
- [39] Newey, W.K. and Powell, J.L. (1987). Asymmetric least squares estimation and testing. *Econometrica*, **55**, 819–847.
- [40] Newey, W.K. and West, K.D. (1987). A simple, positive semi-definite, heteroskedasticity and autocorrelation consistent covariance matrix. *Econometrica*, **55**(3), 703–708.
- [41] Resnick, S. (2007). *Heavy-Tail Phenomena: Probabilistic and Statistical Modeling*. Springer.
- [42] Rootzén, H. and Tajvidi, N. (1997). Extreme value statistics and wind storm losses: a case study. *Scandinavian Actuarial Journal*, **1**, 70–94.
- [43] Scarrott, C. and MacDonald, A. (2012). A review of extreme value threshold estimation and uncertainty quantification. *REVSTAT – Statistical Journal*, **10**(1), 33–60.

- [44] Simiu, E. and Heckert, N.A. (1996). Extreme wind distribution tails: a “peaks over threshold” approach. *Journal of Structural Engineering*, **122**(5), 539–547.
- [45] Wang, S.S. (2004). Cat bond pricing using probability transforms. *Geneva Papers: Etudes et Dossiers*, **278**, 19–29.
- [46] Zimbidis, A.A., Frangos, N.E. and Pantelous, A.A. (2007). Modelling earthquake risk via extreme value theory and pricing the respective catastrophe bonds. *ASTIN Bulletin*, **37**(1), 163–183.